Journal of Integrative Neuroscience

*J. Integr. Neurosci.* **2026**; 25(7): 50711
https://doi.org/10.31083/JIN50711

*Original Research*

# Knockdown of Smox Protects Against Cerebral Ischemia/Reperfusion Injury by Suppressing Neuronal Autophagy via the AKT/AMPK/mTOR Phosphorylation Pathway

Zhihui Li[1,†], Qian Wang[2,3,†], Kaixuan Ma[2,3], Mengna Yu[2,3], Yanyan Wang[4], Zhongqiao Ge[5], Peng Lin[5], Hui Wang[2,3], Lexun Lin[2,3], Yang Chen[2,3], Lina Jia[2,3], Heming Li[2,3], Zhongqiu Fu[6], Zhaohua Zhong[2,3,*], Guangtian Wang[2,3,*]

[1]Department of Neurology, The Fourth Affiliated Hospital of Harbin Medical University, 150086 Harbin, Heilongjiang, China
[2]Teaching Center of Pathogenic Biology, School of Basic Medical Sciences, Harbin Medical University, 150081 Harbin, Heilongjiang, China
[3]Department of Microbiology, School of Basic Medical Sciences, Harbin Medical University, 150081 Harbin, Heilongjiang, China
[4]Teaching Center of Morphology, School of Basic Medical Sciences, Harbin Medical University, 150081 Harbin, Heilongjiang, China
[5]Department of Biochemistry and Molecular Biology, School of Basic Medical Sciences, Harbin Medical University, 150081 Harbin, Heilongjiang, China
[6]Department of Neonatology, Zhuhai Women and Children's Hospital, 519000 Zhuhai, Guangdong, China
*Correspondence: zhongzh@hrbmu.edu.cn (Zhaohua Zhong); wangguangtian0451@163.com (Guangtian Wang)
[†]These authors contributed equally.
Academic Editor: Bettina Platt
Submitted: 4 February 2026 Revised: 16 April 2026 Accepted: 23 April 2026 Published: 27 July 2026

**Abstract**

**Background:** Stroke is a major cause of morbidity and mortality, characterized by neuronal damage and complex cell death pathways. This study aimed to investigate the protective role of spermine oxidase (Smox) in ischemic stroke and its effect on neuronal autophagy. **Methods:** We employed transient middle cerebral artery occlusion (tMCAO) models and oxygen-glucose deprivation/reoxygenation (OGD/R) experiments in HT22 cells to explore the protective effects of Smox knockdown against ischemic injury and to evaluate changes in autophagy. **Results:** Smox levels were significantly elevated following stroke, and correlated with increased autophagic activity and neuronal apoptosis. In contrast, knockdown of Smox reduced neuronal death and improved neurological function while decreasing autophagy activation. Mechanistically, Smox may regulate autophagy via the phosphorylation of protein kinase B (AKT), AMP-activated protein kinase (AMPK), and mechanistic target of rapamycin (mTOR); Smox knockdown increased AKT and mTOR phosphorylation, while reducing AMPK phosphorylation, suggesting a potential shift in the regulation of neuronal autophagy. **Conclusions:** Our findings suggest a dual role for Smox in stroke pathology, indicating that it may influence autophagy via the AKT/AMPK/mTOR signaling, which could be critical for neuronal survival after ischemic injury. Targeting Smox may offer a therapeutic strategy for neuronal protection and recovery in stroke management, suggesting the potential importance of autophagy modulation in ischemic brain injury.

**Keywords:** stroke; spermine oxidase; autophagy; neurons; AKT/AMPK/mTOR signaling pathway

## 1. Introduction

Stroke is a severe cardiovascular disease with high rates of morbidity, disability, and mortality. Cerebral ischemic stroke accounts for more than 80% of stroke cases [1,2]. Currently, the primary approved treatments for acute ischemic stroke include thrombolytic therapy and endovascular mechanical thrombectomy [3,4,5]. When used alone or in conjunction with intravenous thrombolysis (a bridging strategy), endovascular mechanical thrombectomy achieves over 80% recanalization and significantly improves clinical outcomes for ischemic stroke patients with large vessel occlusions in the proximal anterior circulation [6,7]. However, many patients who experience successful recanalization still face early complications, such as secondary infarct growth, symptomatic hemorrhagic transformation, and malignant edema. Approximately 50% of patients remain disabled several months after undergoing endovascular mechanical thrombectomy [8,9]. In addition, the limited treatment window poses challenges in achieving optimal therapeutic outcomes [10]. Therefore, more effective therapies are urgently needed to promote the recovery of ischemic tissue and improve prognosis following a stroke.

Various types of neuronal death can be triggered by a stroke, including apoptosis, autophagy, necroptosis, necrosis, and pyroptosis [11,12,13,14]. Autophagy is a cellular degradation process that helps to maintain normal cellular functions and homeostasis. It plays a role in neurodegenerative diseases by breaking down dysfunctional organelles and proteins [15,16,17,18]. Biomarkers of activated autophagy have been found in the brains of mice with ischemic stroke [19,20]. The role played by autophagy in cerebral ischemia remains controversial, since it has been demonstrated to induce neuronal death but also to protect

against ischemic injury. Some studies suggest that autophagy can be neuroprotective by clearing damaged cellular components and promoting cell survival under stress [19,21]. The dual role of autophagy in stroke highlights its complex regulation and the need for further research to understand its mechanisms and potential for therapy. Determining the effects of autophagy activation could lead to new interventions that reduce neuronal damage and improve recovery after ischemic events.

Spermine oxidase (Smox) is an essential and highly inducible enzyme in the polyamine catabolic pathway that facilitates spermine oxidation to yield spermidine. This is accompanied by deleterious byproducts such as hydrogen peroxide and 3-aminopropanal. In instances of cellular stress, Smox expression is elevated, leading to increased reactive oxygen species (ROS) that can result in cell injury and death [22,23,24]. Spermine is an organic cation characterized by numerous amino groups. It has many biological functions, including immunological control, maintaining mitochondrial homeostasis, promotion of autophagy, and facilitation of cell proliferation and differentiation. Research indicates that irregular spermine metabolism is significantly associated with the initiation and progression of several human diseases [25]. Prior research has demonstrated activation of Smox in gastric epithelial cells (GECs) and myeloid cells following infection with *Helicobacter pylori* (*H. pylori*) in both humans and rats [26]. Smox activity in macrophages facilitates apoptosis and diminishes antibacterial efficacy [27,28], thereby contributing to immunological evasion of *H. pylori.* Moreover, Smox has been demonstrated to cause DNA damage and apoptosis in GECs, with a noted association between Smox expression and the progression of illness in *H. pylori*-infected individuals [29]. A separate study demonstrated that Smox regulates ATG5-mediated autophagy, contributing to kidney senescence and fibrosis [24]. Nonetheless, there is still no direct evidence for the involvement of Smox in autophagy-mediated stroke.

The current study explored the role of Smox in neuronal injury and activation of autophagy. In contrast to the detrimental effects of Smox upregulation, our results indicate that knockdown of Smox provides protection against ischemic injury by suppressing autophagy, as demonstrated in both the transient middle cerebral artery occlusion (tMCAO) mouse model and the oxygen-glucose deprivation/reoxygenation (OGD/R) HT22 cell model. The suppressive effect of Smox knockdown on autophagy may occur through the protein kinase B (AKT)/ AMP-activated protein kinase (AMPK)/ mechanistic target of rapamycin (mTOR) phosphorylation pathway, although further research is necessary to confirm this relationship.

## 2. Material and Methods

### *2.1 Animals*

Male C57BL/6J mice (8-week-old, weighing 20–23 g) were obtained from Liaoning Changsheng Laboratory Animal Co., Ltd (Fushun, Liaoning, China). The animals were given unlimited access to food and water and housed under 12 h:12 h light–dark cycles.

### *2.2 Microinjection of Smox shRNA Lentivirus*

Adult male C57BL/6J mice were anesthetized with isoflurane (R510, RWD Life Science, Shenzhen, Guangdong, China) delivered throughout the procedure via a nose cone (3% for induction and 1.5% for maintenance). The mouse was then placed on a stereotaxic device in the prone position. A 1 cm vertical incision was made, and the bregma was identified as an anatomical landmark. The injection coordinates for the left lateral ventricle were set at 0.3 mm posterior to the bregma, 1.0 mm lateral to the left, and 2.2 mm in depth. After drilling a burr hole, a pre-calibrated microinjection needle was inserted and left in place for 5 min. Smox shRNA lentivirus or control lentivirus (2 μL in total, Hanbio Biotechnology Co., Ltd, Shanghai, China) was then injected into the left lateral ventricle at the rate of 0.1 μL/min. The following sequences were used for shSmox and the negative control (sh-Con): shSmox: 5'-CCGGGCAGTACACCAGTTTCTTTAGTCAAGAGCTAAAGAAACTGGTGTACTGCAAATACAGACTCATGGTAGCTTTTTG-3';sh-Con:5'-CCGGTTCTCCGAACGTGTCACGTTTCAAGAGAACGTGACACGTTCGGAGAATTTTTG-3'. After injection, the needle was left for another 5 min before being slowly withdrawn. The scalp was sterilized, sutured, and the animal was returned to its home cage.

### *2.3 Transient Middle Cerebral Artery Occlusion (tMCAO) and TTC staining*

Ischemic stroke tests were performed on male mice (8-week-old, weight 20–23 g). Anesthesia was induced and maintained as described above. The intraluminal filament method was utilized to generate tMCAO, as previously detailed [30,31]. The suture was affixed and fastened, and the animals recuperated by positioning on a heating pad maintained at 37 °C. After 60 min of ischemia, blood flow was reinstated by excision of the suture, followed by suturing and disinfection of the wound. The animals were subsequently placed within a temperature-regulated enclosure and given access to liquid sustenance, graduating to standard feeding following the restoration of mobility. The mice were randomly allocated to either the Sham or tMCAO groups, with the Sham group undergoing all operations except for suture placement. All surgical operations were performed under sterile settings. To assess cerebral ischemic injury, TTC (2,3,5-triphenyltetrazolium chloride) staining was performed. At 24 h after tMCAO, mice were deeply anesthetized and euthanized. Brains were rapidly removed and coronally sectioned into 1-mm-thick slices using a brain matrix. Slices were incubated in 1% TTC solution at 37 °C for 20 min in the dark, then fixed in 4% paraformaldehyde overnight. Stained slices were photographed with a dig-

ital camera. Infarct areas (unstained white regions) were measured using ImageJ software. Infarct volume (%) was calculated as [(contralateral hemisphere volume) – (ipsilateral hemisphere volume – measured infarct volume)] / (contralateral hemisphere volume) × 100%. Total infarct volume ($mm^3$) was obtained by summing corrected infarct areas across all sections and multiplying by slice thickness (1 mm).

### *2.4 Western Blot*

RIPA lysis buffer (P0013B, Beyotime, Shanghai, China) was used to extract proteins, which were then separated by 10% sodium dodecyl sulfate polyacrylamide gel electrophoresis (PG112, Epizyme, Cambridge, MA, USA). Proteins were subsequently transferred onto polyvinylidene fluoride membranes (TM-PVDF-R-45, LABSELECT, Beijing, China) using established protocols [32,33]. Following incubation with blocking buffer, membranes were incubated overnight at 4 °C with primary antibodies (each diluted 1:1000) against Smox (15052-1-AP, Proteintech), glial fibrillary acidic protein (GFAP, 16825-1-lg, Proteintech, Rosemont, Chicago, USA), Neuronal Nuclei (NeuN, 26975-1-AP, Proteintech, Rosemont, Chicago, USA), Ionized calcium-binding adapter molecule 1 (Iba-1, 66827-1-lg, Proteintech, Rosemont, Chicago, USA), B-cell lymphoma 2 (Bcl-2, 26593-1-AP, Proteintech, Rosemont, Chicago, USA), microtubule-associated protein 1 light chain 3 (LC3B, 381544, Zenbio, Durham, NC, USA), Sequestosome-1 (SQSTM1) (p62, 18420-1-AP, Proteintech, Rosemont, Chicago, USA), Beclin 1 (11306-1-AP, Proteintech, Rosemont, Chicago, USA), AKT (10176-2-AP, Proteintech, Rosemont, Chicago, USA), p-AKT (phosphorylated protein kinase B, 28731-1-AP, Proteintech, Rosemont, Chicago, USA), AMPK (10929-2-AP, Proteintech, Rosemont, Chicago, USA), p-AMPK (80209-6-RR, Proteintech, Rosemont, Chicago, USA), mTOR (R380411, Zenbio), p-mTOR (381557, Zenbio), or β-actin (66009-1-lg, Proteintech). They were further treated with HRP-conjugated affinipure goat anti-mouse or anti-rabbit IgG (H + L) secondary antibody (1:2000, SA00001-1 or SA00001-2, Proteintech, Rosemont, Chicago, USA). Signals were identified using an automated chemiluminescence image analysis system (GE600, General Electric Company, Boston, MA, USA). Individual protein bands were analyzed by densitometry with ImageJ Fiji software (NIH, Bethesda, USA).

### *2.5 Immunofluorescence*

Cells were fixed with 4% paraformaldehyde (P0099-500ml, Beyotime), permeabilized with 0.3% Triton X-100 (C0265, Beyotime), then incubated overnight at 4 °C with primary antibody against LC3B (1:100, 381544, Zenbio). Slides were then mounted and photographs recorded using a fluorescence microscope(C2, Nikon, Minato, Tokyo, Japan). Brain samples were cut into coronal slices (30 µm) and treated for 15 min with 0.3% Triton X-100 in PBS (Beyotime, P0096-100) prior to tissue staining. Sections were subsequently incubated for 60 min at ambient temperature with 10% goat serum (C0265, Beyotime) in 0.3% Triton X-100. Frozen brain slices were then treated overnight at 4 °C with Iba-1 (016-26721, Wako, Osaka, Japan), NeuN (ab104224, Abcam, Cambridge, UK), and GFAP (G3893-2ml, Sigma-Aldrich, St. Louis, Missouri, USA), followed by a 1 h incubation at room temperature with either Alexa Fluor™ 488 goat anti-mouse antibody (1:250; Invitrogen, Waltham, MA, USA), Alexa Fluor™ 594 goat anti-rabbit antibody (1:250; Invitrogen), or Alexa Fluor™ 488 goat anti-rat antibody (1:250; Invitrogen). Following a final wash in PBS, slices were affixed to glass slides and images recorded with a confocal microscope (C2, Nikon).

### *2.6 Quantitative Real-Time PCR*

TRIzol reagent (15596026CN, Invitrogen, Waltham, MA, USA) was used to extract total mRNA from brain tissue, as previously described [34,35]. cDNA was generated from mRNA with an M-MLV reverse transcriptase kit (R323, Vazyme, Nanjing, Jiangsu, China) and 1 µg of total RNA. qRT-PCR with SYBR Green PCR master mix (R323, Vazyme) was used to evaluate mRNA levels with the StepOnePlus™ Real-time PCR System (Q711,Vazyme). The primers used are shown in **Supplementary Table 1**. *GAPDH* was utilized as the reference gene (Sangon Biotech, Shanghai, China), and relative levels of gene expression were estimated with the comparable cycle threshold approach.

### *2.7 Cell Culture*

HT22 cells (Wuhan Sainuo Biotechnology Co., Ltd., Wuhan, Hubei, China) were maintained in DMEM medium (Beyotime, C0891-500ml) containing 10% fetal bovine serum (Sangon, E510002-0500, Shanghai, China) and 1% penicillin/streptomycin (Beyotime, C0222). The medium was replenished every second day. For immunofluorescence staining, $2 \times 10^4$ cells per well were seeded into a transwell 24-well plate. The cell line used in this research was not passaged more than 25 times. The cell line has been validated through surface marker analysis, and mycoplasma testing was performed in our laboratory using a PCR-based method, and results confirm the cells are free from contamination.

### *2.8 Oxygen–Glucose Deprivation and Reoxygenation (OGD/R)*

HT22 cells from various groups were cultured in a 6-well plate until they achieved confluence, then washed with PBS. To conduct the OGD/R tests, cells were subsequently incubated for 6 h at 37 °C in DMEM without glucose and in a hypoxic incubator containing 95% $N_2$ and 5% $CO_2$. After the OGD phase, complete culture medium with 95% air and 5% $CO_2$ was then used to reoxygenate

the cells for 24 h, followed by harvesting. Control cells were grown at 37 °C in full culture medium and exposed to 5% $CO_2$ and 95% air throughout the experiment. They were subjected to identical washing and medium changes as the OGD/R cells. For pharmacological inhibition experiments, following Smox knockdown by sh-Smox transfection, HT22 cells were treated with GSK690693 (25 μM) for 2 h. GSK690693 (HY-10249, MedChemExpress, Monmouth Junction, NJ, USA) was dissolved in DMSO as a stock solution and diluted in culture medium to the working concentration. Control cells received an equivalent volume of DMSO (final concentration ≤0.1%, v/v).

*2.9 CCK-8 Assay*

Cells from the hippocampal neuronal cell line HT22 were seeded into 96-well plates at $2 \times 10^4$ cells/well. After being subjected to OGD/R treatment, CCK-8 reagent (C0038, Beyotime) was added to the cells (10 μL per well) and incubated at 37 °C for 3 h. Optical density at 450 nm was then measured using a microplate reader. A higher absorbance ratio relative to the controls indicated greater cell viability.

*2.10 Transmission Electron Microscopy (TEM)*

HT22 cells were fixed in 2.5% glutaraldehyde (G5882, Sigma-Aldrich) for 12 h at 4 °C, post-fixed in 1% osmium tetroxide (O302601, Aladdin, Shanghai, China), dehydrated in graded ethanol (E809064, Macklin, Shanghai, China) and propylene oxide (W611187, Energy Chemical, Shanghai, China), embedded in epoxy resin (E8000, Beijing Haide Biotech Co., Ltd., Beijing, China), then polymerized at 60 °C for 48 h. Semi-thin sections (1.0 μm) were observed after staining with toluidine blue (T104232, Aladdin). Ultra-thin sections were examined by TEM after staining with 2% uranyl acetate (csw01, Hubei Chushengwei Chemical Co., Ltd, Wuhan, Hubei, China) and lead citrate (DJ152, Kuafu Lab, Beijing, China), and subsequently photographed with a Hitachi HT7700 transmission electron microscope (Hitachi, Chiyoda, Tokyo, Japan).

*2.11 Nissl Staining*

Following euthanasia of mice by intraperitoneal injection of sodium pentobarbital (150 mg/kg) and subsequent cervical dislocation to ensure death, a thoracotomy was performed as per the tMCAO procedure. A needle was introduced into the apex of the left ventricle to gradually perfuse the heart with 100 mL of a pre-cooled saline solution. This was followed by steady infusion with 50 mL of 4% paraformaldehyde for internal fixation. The skull was subsequently opened and the intact brain tissue was removed and externally fixed in 4% paraformaldehyde. Brain tissue was submerged first in 20% sucrose in distilled water and then 30% sucrose in distilled water and stored overnight in a refrigerator at 4 °C. Once it had fully submerged, the brain tissue was removed, embedded in optimum cutting temperature (OCT) compound, and cut into 30 μm sections with a cryostat (TSX50086LA, Thermo Fisher Scientific, Waltham, MA, USA). These were stained with the Nissl staining kit (Cat# C0117, Beyotime) as recommended by the manufacturer. The brain sections were then mounted with neutral gum and examined by optical microscopy. Up to three sections were prepared for each mouse, and four fields were acquired from each section of the prefrontal cortex.

*2.12 TUNEL Staining*

TdT enzyme was combined at a 1:9 ratio with fluorescent labeling solution from the terminal deoxynucleotidyl transferase dUTP nick end labeling (TUNEL) assay kit (Cat#C1089, Beyotime) to formulate TUNEL detection solution. This was administered to a specified area in the tissue and incubated at 37 °C for 1 h. After rinsing three times with PBS (5 min each), 4′,6-diamidino-2-phenylindole (DAPI) dye solution was added to the area and the sections were incubated for 10 min at room temperature in the absence of light. Tissue sections were then examined by fluorescence microscopy and the images recorded (C2, Nikon). Four areas were investigated from each cortical slice, with up to three sections obtained from each mouse for each protocol.

*2.13 Measurement of Neurological Deficits*

The neurological deficit test was conducted 14 days after tMCAO by an investigator who was blinded to the identity of the experimental groups. A modified neurological severity score (mNSS) test was used to assess neurological function [36]. Scores were assigned on a scale from 0 to 14, with 0 indicating normal function and 14 indicating maximum severity. One point was given for the inability to complete a specific test, or for the absence of a tested reflex. Scores between 10–14 indicated severe injury, 5–9 indicated moderate injury, and 1–4 indicated mild injury. The 14-day time point was selected because functional outcomes have typically stabilized by then, allowing reliable evaluation of treatment efficacy.

*2.14 Mouse Behavioral Tests*

An independent investigator blinded to the identity of experimental groups conducted the mouse behavioral tests, with data analysis performed by a separate investigator. Behavioral assessments were performed 14 days after tMCAO. This time point is widely used to evaluate chronic functional recovery, and also aligns with the molecular assessments performed in the current study. The cylinder test [37] was conducted by positioning the mice within a plastic cylinder (15 cm height, 10 cm diameter) and video recording for 5 min. The formula used to calculate the score was: number of right forelimb contacts number of left forelimb contacts/total number of forelimb contacts. This included both the right and left limbs. In the adhesive removal so-

matosensory test [36,38], small adhesive-backed paper dots (25 $mm^2$) serving as bilateral tactile stimuli were placed on the distal-radial area of each forelimb. The time required for mice to eliminate each stimulus was documented during three daily sessions, with a minimum period of 5 min between each trial. Before the procedure, the animals participated in a 3-day training regimen. The results were calculated as the disparity in duration of removal (in seconds) between the left and right forelimbs.

### *2.15 Molecular Docking*

To investigate the potential binding interactions between Smox and AKT, AMPK, and mTOR, protein–protein molecular docking simulations were performed in this study using the HDOCK server (http://hdock.phys.hust.edu.cn/). The three-dimensional structures of Smox, AKT, AMPK, and mTOR were obtained from the Protein Data Bank (https://www.rcsb.org). Appropriate models were selected for visualization analysis by combining the template modeling results and free docking results provided by HDOCK. PyMOL 2.5.x software (Schrödinger Inc, New York, NT, USA) was used to characterize the key residues and hydrogen-bond networks at the interaction interface.

### *2.16 Statistical Analysis*

All experiments were performed at least in triplicate. The Student's *t*-test was used for statistical comparisons between two groups, and the Mann-Whitney U test for non-normally distributed data. One-way analysis of variance (ANOVA) and Tukey's post-hoc test were employed to compare three or more groups with a single variable. To compare two or more variables across multiple groups, two-way ANOVA and the Holm-Sidak post-hoc test were utilized. A $p$-value of $<0.05$ was considered statistically significant. GraphPad Prism 9.0 (GraphPad Software, Inc., San Diego, California, USA) was utilized for data analysis, with results presented as the mean ± SEM.

## 3. Results

### *3.1 Smox Knockdown Improves Neurological Impairment Following Ischemia in Mice*

Prior studies have established that inhibition of Smox may mitigate neuroinflammation following localized ischemic stroke [39]. In the current investigation, we observed increased levels of Smox in the mouse brain at 24 h post-tMCAO reperfusion (Fig. 1A,B). We subsequently investigated the *in vivo* function of Smox in the etiology of stroke. The lateral ventricles of mice were microinjected with either Control shRNA lentivirus (sh-Con) or Smox shRNA lentivirus (sh-Smox). The effectiveness of shRNA Smox lentivirus knockdown *in vivo* was assessed three weeks post-lentivirus microinjection. Smox expression was markedly reduced in the Smox shRNA-injected animals relative to the Con shRNA-injected group (Fig. 1C,D). The mice underwent tMCAO three weeks post-lentivirus microinjection. TTC staining was conducted to quantify the brain infarct volume 24 h post-surgery. The infarct volume was markedly reduced in Smox shRNA-injected mice (tMCAO-sh-Smox) compared to Control shRNA-injected mice (tMCAO-sh-Con) (Fig. 1E,F). We next assessed the function of Smox by examining neuronal impairments following stroke. After 14 day of tMCAO, neurological impairments were markedly decreased in tMCAO-sh-Smox mice compared to tMCAO-sh-Con mice (Fig. 1G). Assessments of neurological deficit, the adhesive removal test, and the cylinder test were performed 14 days post-tMCAO. Microinjection of the Smox shRNA lentivirus markedly enhanced neurological functions and increased somatosensory capabilities following tMCAO, as seen by the cylinder test and adhesive removal test (Fig. 1H,I). In accordance with these behavioral enhancements, the reduction of Smox expression during tMCAO markedly alleviated neurological impairments and enhanced somatosensory capabilities post-tMCAO. The original Western blot images are available in the **Supplementary Materials**.

### *3.2 Differential Expression of Smox by Brain Cell Types After tMCAO*

Using an immunofluorescence assay, we next examined the role of Smox during acute cerebral ischemia in neurons, astrocytes, and microglia by analyzing brain sections from the cortical areas after tMCAO. Smox was predominantly expressed in $NeuN^+$ neurons, with lower expression in $GFAP^+$ astrocytes and Iba-$1^+$ microglia (Fig. 2A–D). Knockdown of Smox significantly reduced its expression in the tMCAO brain. Furthermore, a notable reduction was observed in the co-localization of $NeuN^+$/$Smox^+$ in tMCAO-sh-Smox mice compared to tMCAO-sh-Con mice. Although GFAP and Iba-1 expression decreased in tMCAO-sh-Smox mice, co-localization of $GFAP^+$/$Smox^+$ and Iba-$1^+$/$Smox^+$ was not significantly different between the tMCAO-sh-Smox group and tMCAO-sh-Con group. We also explored the regulatory effects of Smox knockdown on neurons, microglia, and astrocytes by measuring expression levels of the characteristic markers NeuN, Iba-1, and GFAP using Western blot analysis. As shown in Fig. 2E–H (the original Western blot images are available in the **Supplementary Materials**), knockdown of Smox increased NeuN expression while decreasing Iba-1 expression in the ischemic hemisphere of tMCAO mice compared to tMCAO-sh-Con mice. Conversely, knockdown of Smox had less effect on GFAP expression, as indicated by combining the immunofluorescence and Western blot results, suggesting beneficial effects on neurons. These findings indicate that, following tMCAO, NeuN predominantly expressed Smox. Accordingly, the subsequent experiments focused specifically on neuronal cells.

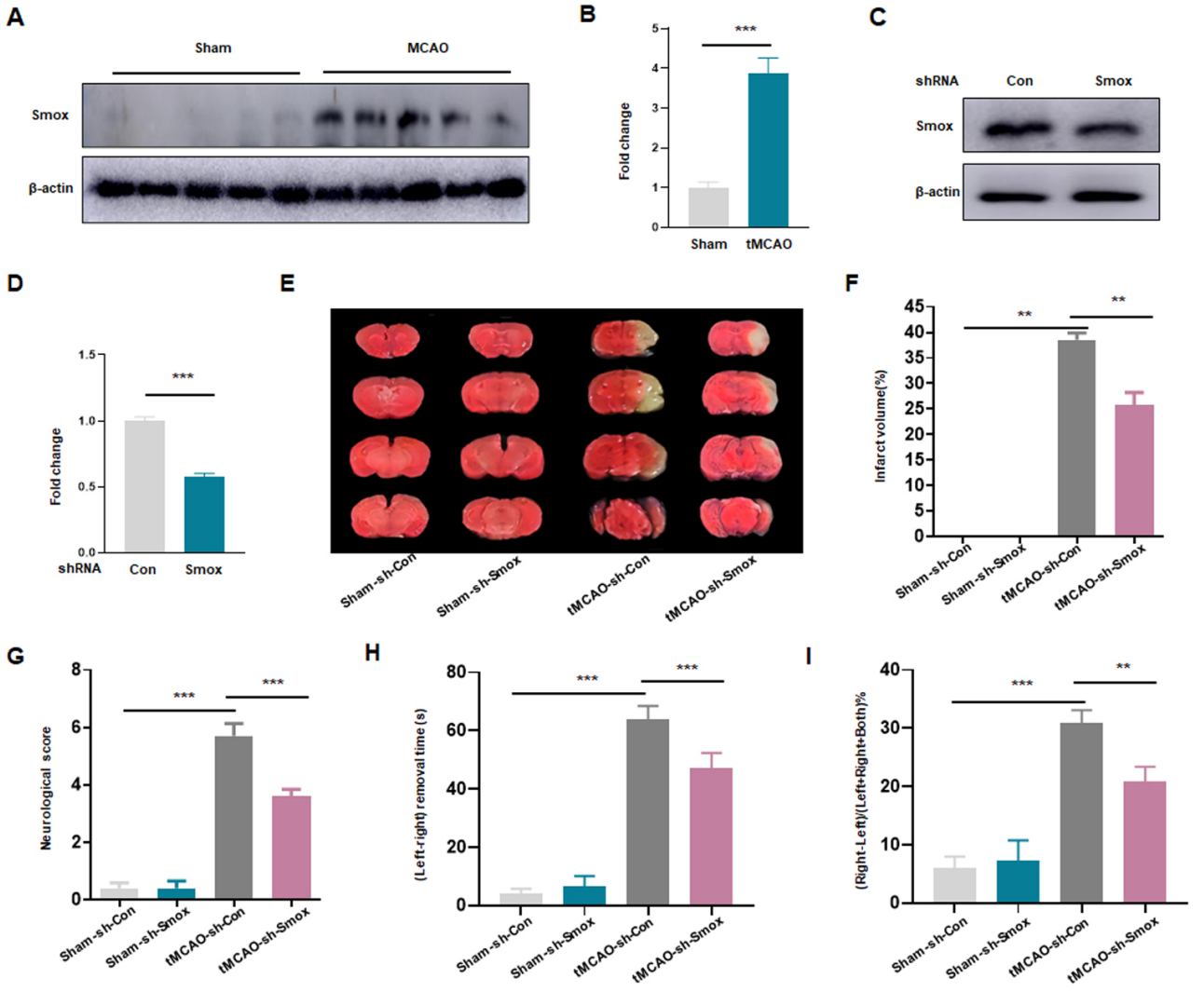


**Fig. 1. Knockdown of Smox improves the neuroprotective effect after tMCAO**. (A,B) Western blot analysis was used to evaluate Smox expression in the Sham and tMCAO groups. $n = 5$. (C,D) The knockdown efficiency of Smox expression after Smox shRNA lentivirus microinjection was determined by quantifying Smox expression at 3 weeks after microinjection through Western blot analysis. $n = 3$. (E) Representative images of TTC stained brain slices on 1 days after tMCAO. $n = 5$. (F) Quantitative analysis of brain infarct volumes. $n = 5$. (G–I) The mNSS, adhesive removal and cylinder test were performed on day 14 post tMCAO. $n = 5$. $^{**}p < 0.01$, $^{***}p < 0.001$. Con, control; Smox, spermine oxidase. tMCAO, transient middle cerebral artery occlusion; TTC, 2,3,5-Triphenyltetrazolium chloride.

### *3.3 Knockdown of Smox Inhibits Neuronal Apoptosis Induced by tMCAO*

Double labeling with NeuN and TUNEL was conducted to evaluate cortical neuronal death in the infarct region five days post-tMCAO. Compared to the sham mice, ischemic injury led to considerable neuronal apoptosis. However, sh-Smox enhanced neuronal survival, thereby demonstrating the efficient anti-apoptotic properties of sh-Smox treatment (Fig. 3A,B). Western blot assay showed upregulation of Bcl-2-associated X protein (Bax) expression and downregulation of Bcl-2 expression in the tMCAO-sh-Con group. Knockdown of Smox suppressed Bax expression and increased Bcl-2 expression (Fig. 3C,D, the original Western blot images are available in the **Supplementary Materials**). Nerve cell morphology was normal in the sham group, with Nissl bodies observable by Nissl staining. Neuronal loss was observed in tMCAO-sh-Con mice. This was characterized by nuclear pyknosis and indistinct Nissl body structure, indicating neuronal degeneration. In comparison to the tMCAO-sh-Con group, knockdown of Smox increased the number of surviving neurons with discernible Nissl bodies, indicative of neuronal regeneration (Fig. 3E). These findings indicate that Smox knockdown reduces neuronal death in the ischemic cerebral cortex.

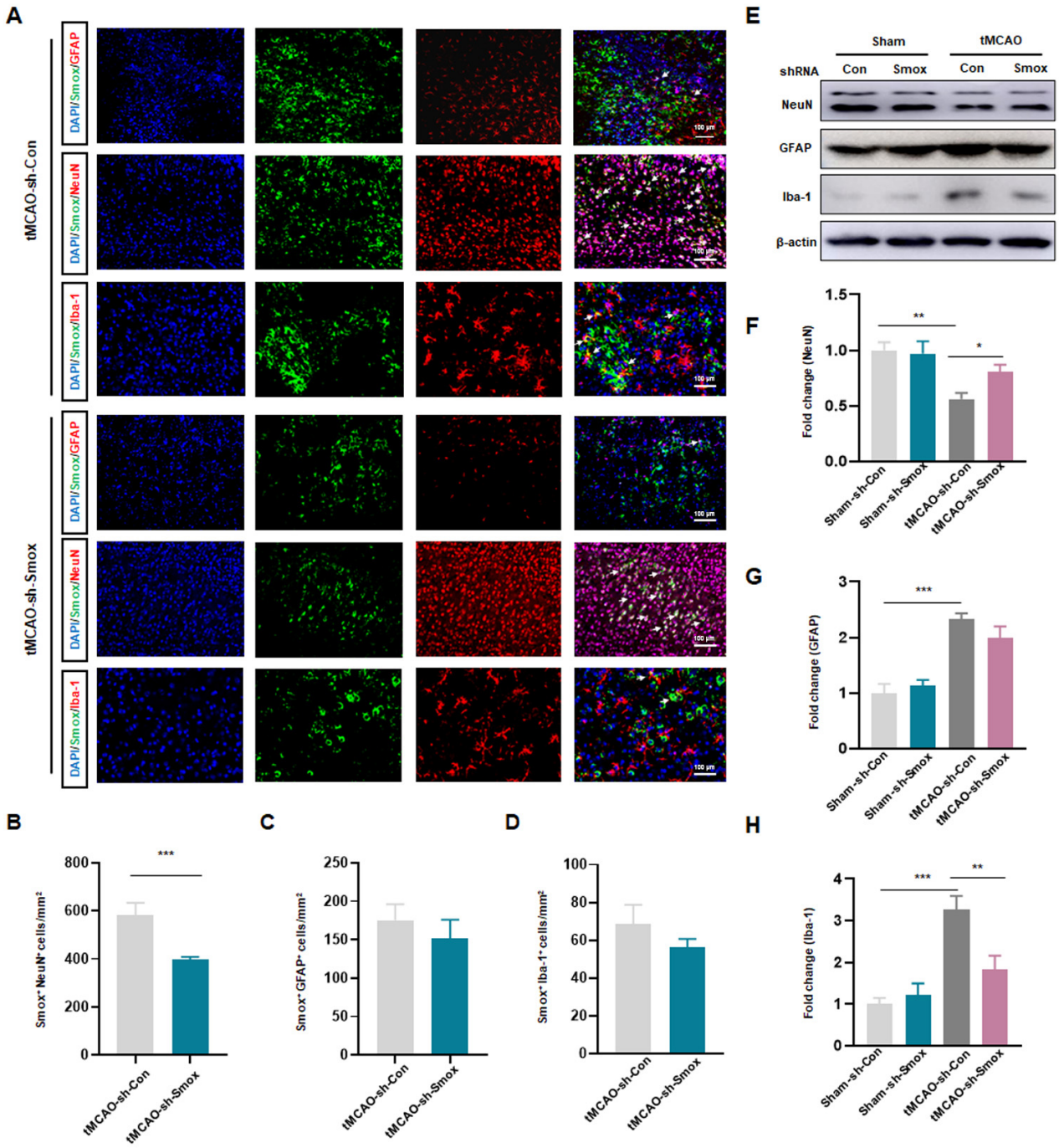


**Fig. 2. Differential expression of Smox by brain cell types after tMCAO**. (A) Immunofluorescence images showing Smox (green) with NeuN (red, neurons), Iba-1 (red, microglia), or GFAP (red, astrocytes) in tMCAO-sh-Con and tMCAO-sh-Smox groups at 24 h post-reperfusion. Arrows indicate co-localization. Scale bar = 100 μm. (B–D) Quantification of $NeuN^+/Smox^+$, $GFAP^+/Smox^+$, and $Iba\text{-}1^+/Smox^+$ cells. (E–H) NeuN, GFAP, and Iba-1 protein expression levels were quantified in the ischemic hemisphere of tMCAO mice. $n = 3$. $^*p < 0.05$, $^{**}p < 0.01$, and $^{***}p < 0.001$. NeuN, Neuronal Nuclei; Iba-1, Ionized calcium-binding adapter molecule 1; GFAP, glial fibrillary acidic protein.

### *3.4 Smox Knockdown Represses Autophagy In Vivo Following tMCAO*

After validating the protective capacity of Smox in tMCAO, we further examined whether it modulates neuronal apoptosis via autophagy. We assessed the impact of tMCAO on the levels of autophagic proteins and autophagic activity post-stroke by measuring expression of the autophagy-related proteins Beclin 1, p62, and LC3B. In contrast to the sham group, the expression of Beclin 1 and LC3B II/I was markedly elevated in the tMCAO group

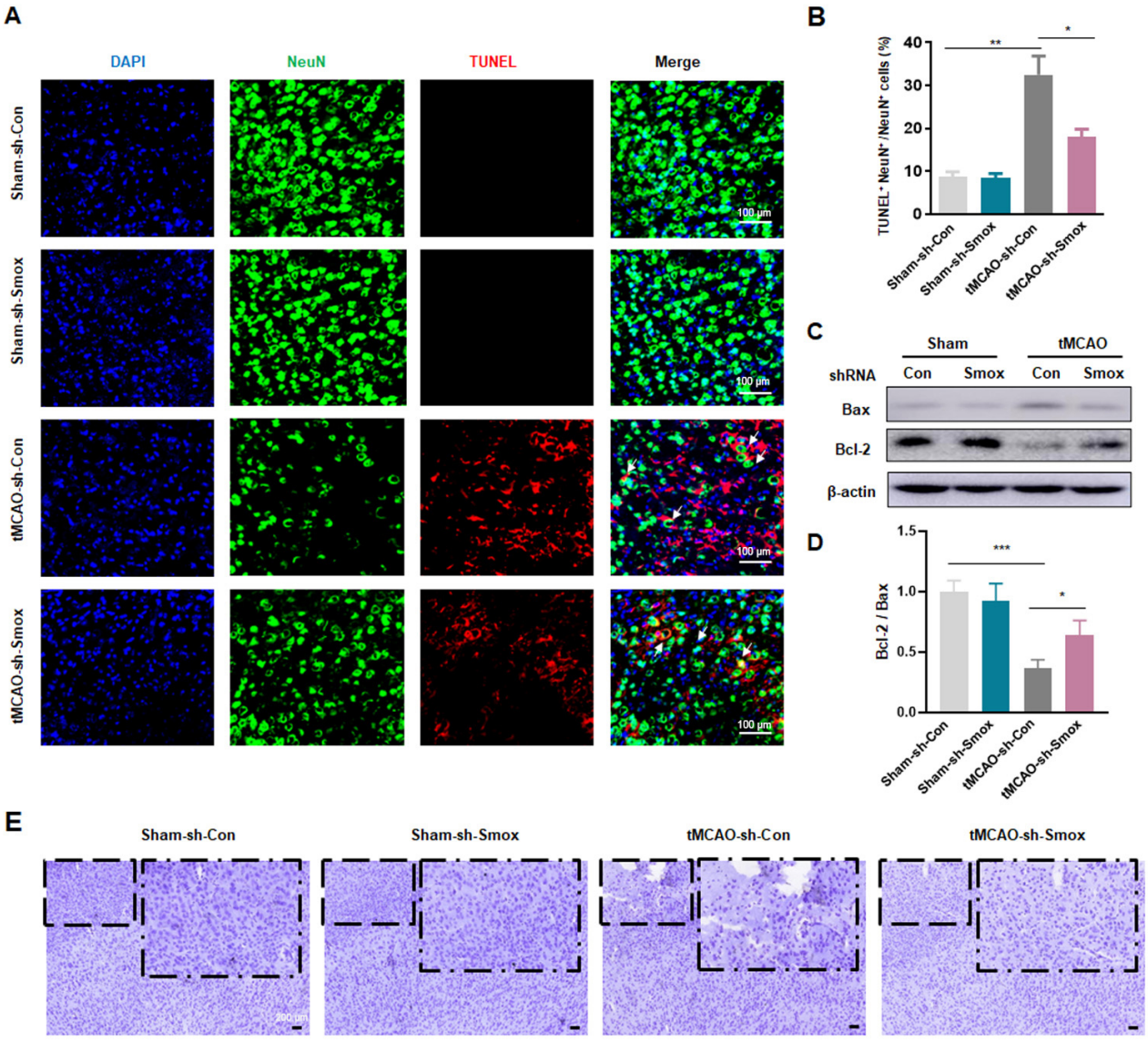


**Fig. 3. Knockdown of Smox suppresses neuronal apoptosis in the ischemic cerebral cortex**. (A) Representative TUNEL staining images of cortical neurons. Apoptotic neurons are identified by the co-localization of TUNEL (red) and NeuN (green), as indicated by the arrows. Scale bar = 100 μm. (B) Quantitative analyses of the rate of neuronal apoptosis in each group. $n = 4$. (C) Representative Western blot results of Bax and Bcl-2 expression in the cortex. (D) Quantitative analysis of Bcl-2/Bax ratio, as analyzed by Western blot. $n = 3$. (E) Nissl staining of brain tissue in each group. Scale bar = 200 μm. $^{*}p < 0.05$, $^{**}p < 0.01$, $^{***}p < 0.001$. Bax, Bcl-2-associated X protein; Bcl-2, B-cell lymphoma 2. TUNEL, terminal deoxynucleotidyl transferase dUTP nick end labeling.

(Fig. 4A–D, the original Western blot images are available in the **Supplementary Materials**). However, this increase was attenuated by knockdown of Smox. Furthermore, p62 levels diminished post-stroke, and Smox knockdown mitigated the tMCAO-induced reduction of p62. At the transcriptional level, qPCR analysis showed markedly elevated levels of *Atg5*, *Beclin 1*, and *LC3B* mRNA in the tMCAO group, whereas *p62* levels were diminished, indicating activated autophagy. *Smox* knockdown decreased the *Atg5*, *LC3B*, and *Beclin 1* mRNA levels and increased the *p62* mRNA level (Fig. 4E–H). Immunofluorescence staining confirmed that *LC3B* expression in the cortical penumbra was markedly elevated post-stroke, but this was significantly reduced by *Smox* knockdown. These results demonstrate that autophagy was initiated after the stroke, and Smox could effectively mitigate this post-stroke autophagy activation, thereby providing a neuroprotective effect.

### *3.5 Knockdown of Smox in HT22 Cells Affects Autophagy Following OGD/R*

Autophagy is a crucial signaling pathway in hypoxic and ischemic conditions. We therefore investigated the influence of Smox on this pathway following OGD/R in HT22 cells. These were transfected with either control

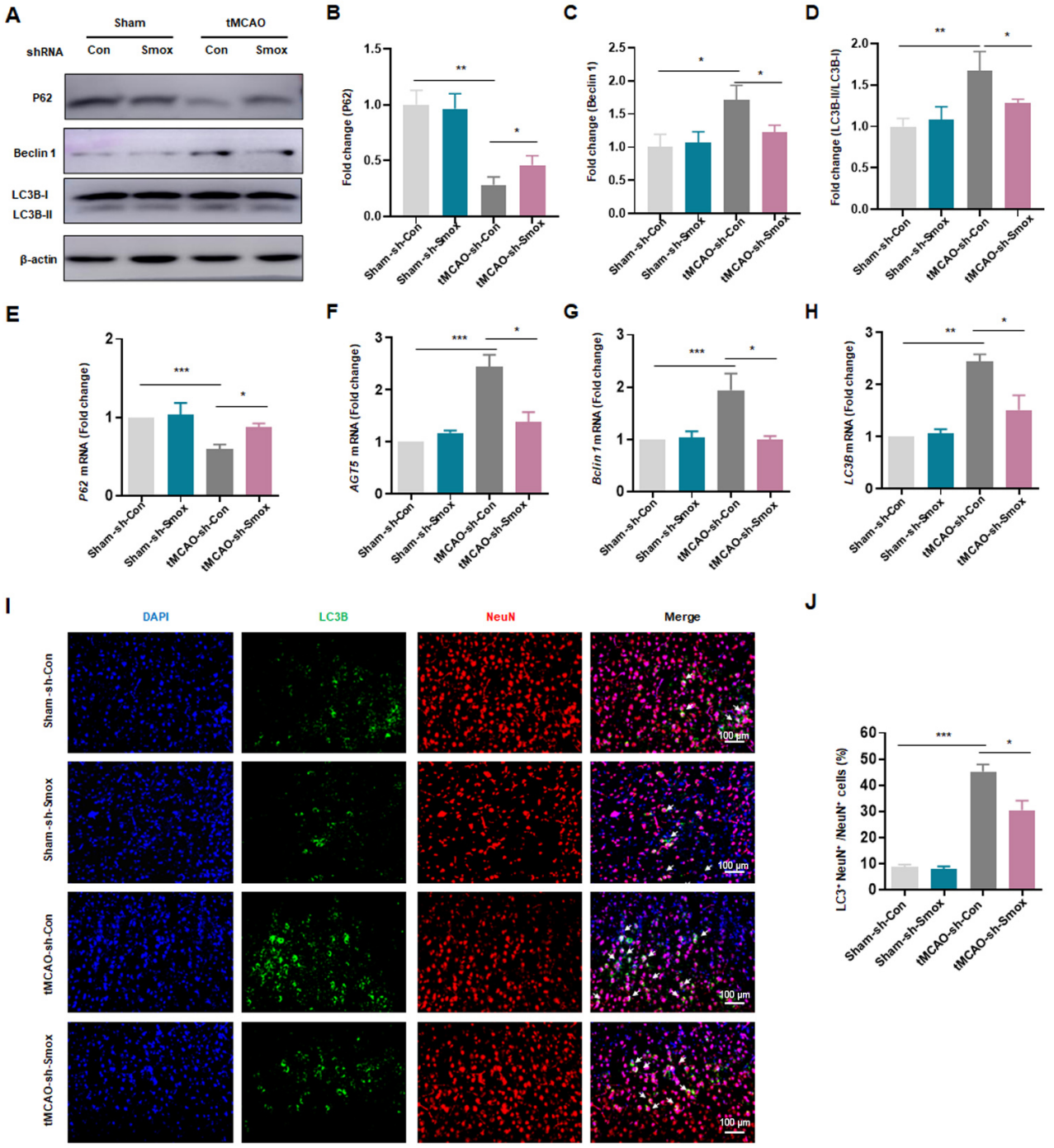


**Fig. 4. Knockdown of Smox inhibits tMCAO-induced autophagy**. (A–D) The effect of Smox on the protein expression levels of p62, Beclin1 and LC3B II/I. $n = 3$. (E–H) The effect of *Smox* on the mRNA expression levels of *p62*, *Atg5*, *Beclin 1* and *LC3B*. $n = 3$. The relative expression levels were normalized to GAPDH. (I,J) Double immunofluorescence staining was performed to detect LC3B (green) and NeuN (red) in the cortical penumbra. Arrows indicate co-localization of LC3B with NeuN. Scale bar = 100 μm. $n = 4$. $^{*}p < 0.05$, $^{**}p < 0.01$, and $^{***}p < 0.001$. p62, Sequestosome-1 (SQSTM1); LC3B, microtubule-associated protein 1 light chain 3 beta.

shRNA lentivirus or Smox shRNA lentivirus and subsequently exposed to OGD/R conditions. Western blot analysis revealed that induction of autophagy due to OGD/R was accompanied by increased LC3B II/I and Beclin 1 protein levels, as determined by, along with decreased p62. Furthermore, knockdown of Smox reversed the increase in LC3B II/I and the decrease in p62 observed in the OGD group (Fig. 5A–D, the original Western blot images are available in the **Supplementary Materials**). The increase in immunoreactive LC3B due to OGD/R was counteracted

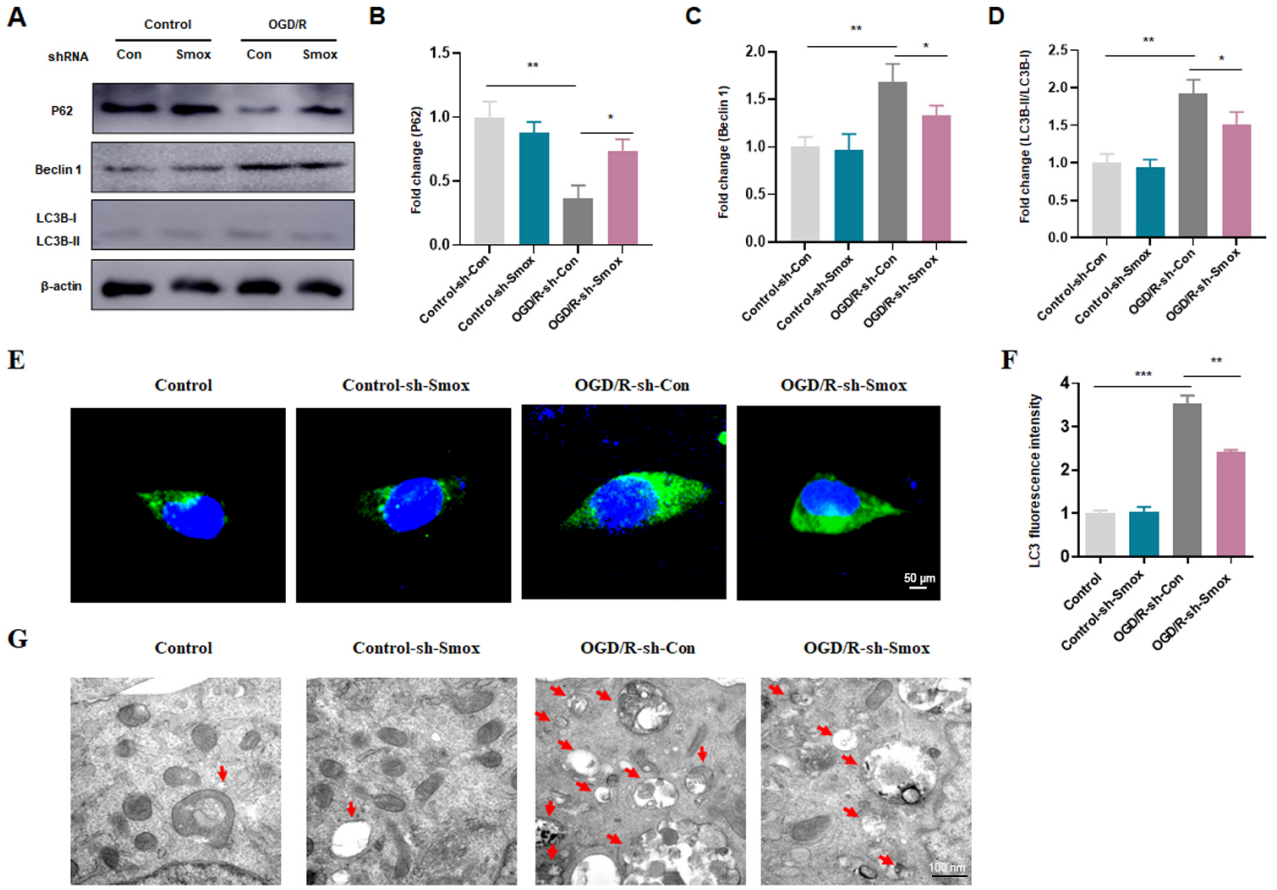


**Fig. 5. Knockdown of Smox in HT22 cells inhibits autophagy induced by OGD/R damage**. (A–D) Representative immunoblots of p62, Beclin 1, and LC3B II/I expression in cultured HT22 cells. n = 3. (E,F) Immunofluorescent staining for LC3B was conducted in each of the different experimental groups. Scale bar = 50 μm. n = 3. (G) Transmission electron microscopy images of autolysosomes (arrows) and double-membraned autophagosomes (arrow heads) in HT22 cells. Scale bar = 100 nm. $^{*}p < 0.05$, $^{**}p < 0.01$, and $^{***}p < 0.001$. OGD/R, oxygen-glucose deprivation/reoxygenation.

by Smox knockdown, as depicted in Fig. 5E,F. These findings suggest that Smox regulates LC3B accumulation *in vitro*. Electron microscopy revealed a significant accumulation of autolysosomes in HT22 cells following OGD/R, which was prevented by Smox knockdown treatment (Fig. 5G). These findings indicate that knockdown of Smox impedes the hypoxia-induced activation of autophagy in HT22 cells.

### *3.6 3-MA and Rapamycin Regulate Autophagy in OGD/R-Induced HT22 Cell Injury*

Smox appears to play a crucial role in regulating neuronal apoptosis, prompting us to examine the involvement of autophagy in this process. The classic autophagy regulators 3-methyladenine (3-MA) and rapamycin were investigated in relation to autophagy and neuronal apoptosis following a stroke. The exposure of HT22 cells to 3-MA at concentrations of 5–10 mM for 24 h resulted in decreased cell viability compared to the controls (**Supplementary Fig. 1A**). Moreover, cell viability was significantly greater in the group treated with 2.5 mM 3-MA than in the OGD/R group (**Supplementary Fig. 1B**). Similarly, rapamycin treatment at 250–1000 nM for 24 h significantly reduced cell viability compared to the controls (**Supplementary Fig. 1C**). Cell viability in the 250 nM rapamycin group was also lower compared with the OGD/R group (**Supplementary Fig. 1D**). The expression of LC3B II/I and NeuN proteins in HT22 cells was assessed by Western blot analysis to investigate the effects of 3-MA (2.5 mM) and rapamycin (250 nM) on autophagy regulation and OGD/R-induced damage. Pretreatment with 3-MA diminished OGD/R-induced LC3B II/I expression and increased NeuN expression in HT22 cells (Fig. 6A–C), while pretreatment with rapamycin enhanced OGD/R-induced LC3B II/I expression and decreased in NeuN expression (Fig. 6D–F). Moreover, 3-MA pretreatment decreased the OGD/R-induced expression of Baxand increased Bcl-2 expression (Fig. 6G,H), whereas rapamycin pretreatment enhanced the OGD/R-induced expression of Bax and reduced Bcl-2 expression (Fig. 6I,J). These findings indicate that both 3-

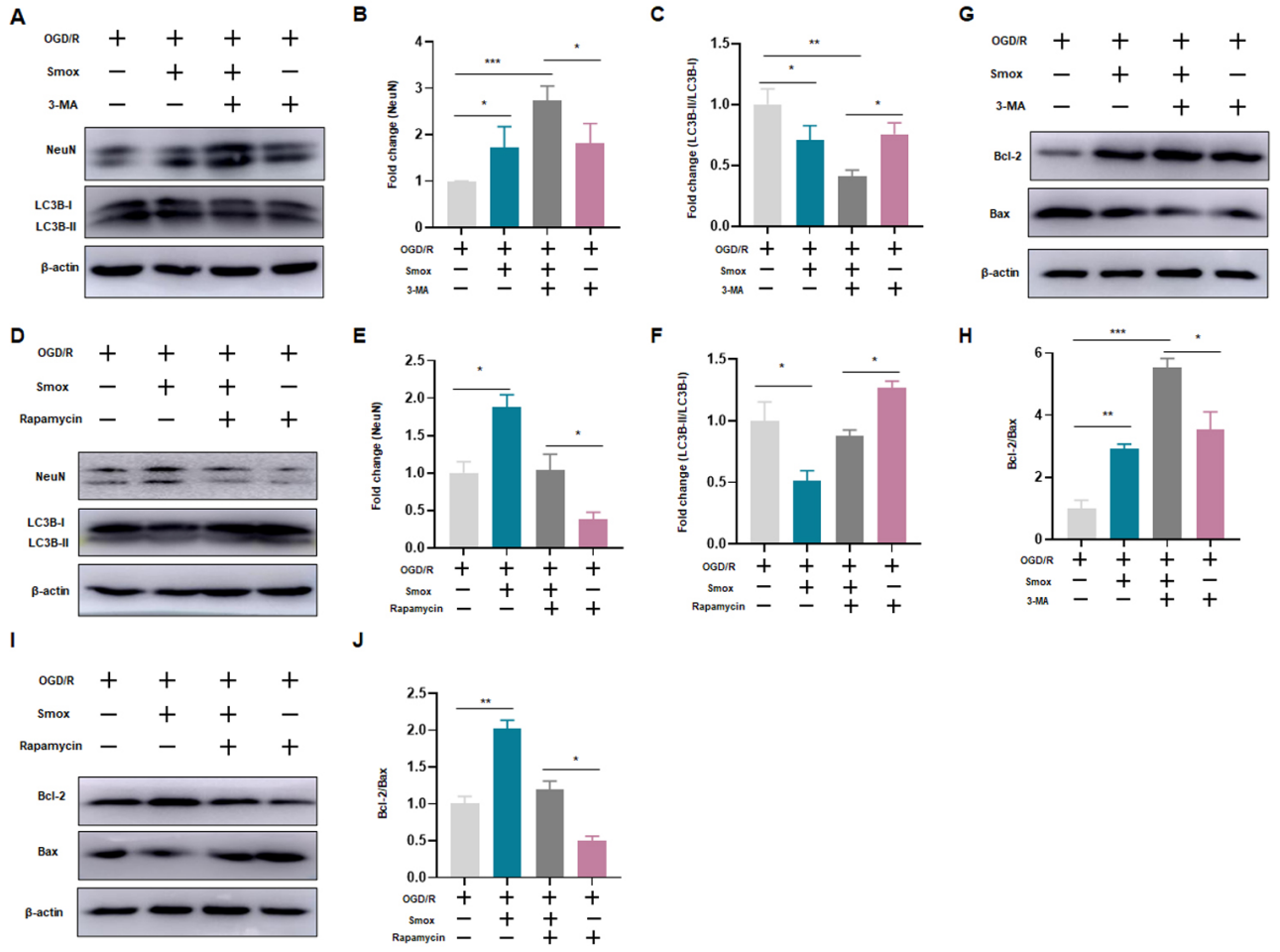


**Fig. 6. Effects of 3-MA and rapamycin on autophagy in OGD/R-induced HT22 cell injury**. HT22 cells were treated for 9 h with 3-MA (2.5 mM) or rapamycin (250 nM) after OGD/R. (A–C) Effects of 3-MA on the levels of LC3B II/I and NeuN protein expression. $n = 3$. (D–F) Effects of rapamycin on the levels of LC3B II/I and NeuN protein expression. $n = 3$. (G,H) Effects of 3-MA on the levels of Bax and Bcl-2 protein expression. n = 3. (I,J) Effects of rapamycin on the levels of Bax and Bcl-2 protein expression. $n = 3$. $^{*}p < 0.05$, $^{**}p < 0.01$, and $^{***}p < 0.001$. 3-MA, 3-Methyladenine.

MA and rapamycin can modulate autophagy, thereby influencing OGD/R-induced neuronal cell injury. The original Western blot images are available in the **Supplementary Materials**.

### *3.7 Smox Regulates AKT/AMPK/mTOR Pathway in Cerebral I/R Injury*

We next investigated the molecular mechanism involving Smox in stroke. Molecular docking was conducted with AutoDock software to analyze interactions between the AKT/AMPK/mTOR pathway and Smox (Fig. 7). Interactions between Smox and AKT, AMPK, or mTOR complexes were further analyzed through molecular dynamics simulations (Fig. 7A–C). In addition, the expression ratios of p-AKT/AKT and p-mTOR/mTOR decreased, while the p-AMPK/AMPK ratio increased following tMCAO, with the phosphorylation sites identified as Thr172, Ser473, and Ser2448 for AMPK, AKT, and mTOR, respectively (Fig. 7D–G, the original Western blot images are available in the **Supplementary Materials**). Silencing of Smox significantly enhanced these effects, indicating it plays a role in the protective mechanisms involving the AKT/AMPK/mTOR pathway against tMCAO damage.

### *3.8 Silencing of Smox Regulates the Phosphorylation Pathway for AKT/AMPK/ mTOR in HT22 Cells Challenged With OGD/R*

Next, the AKT/AMPK inhibitor GSK690693 was used to confirm the involvement of phosphorylated AKT, AMPK, and mTOR in the anti-autophagy effect that knockdown of Smox confers against ischemic brain damage. Treatment with GSK690693 (25 μM) effectively prevented the increased levels of p-AKT, p-mTOR, and decreased p-AMPK induced by Smox silencing in the OGD/R model (Fig. 8A–D). These findings demonstrate that GSK690693 can reverse the effects of p-AKT, p-AMPK, and p-mTOR

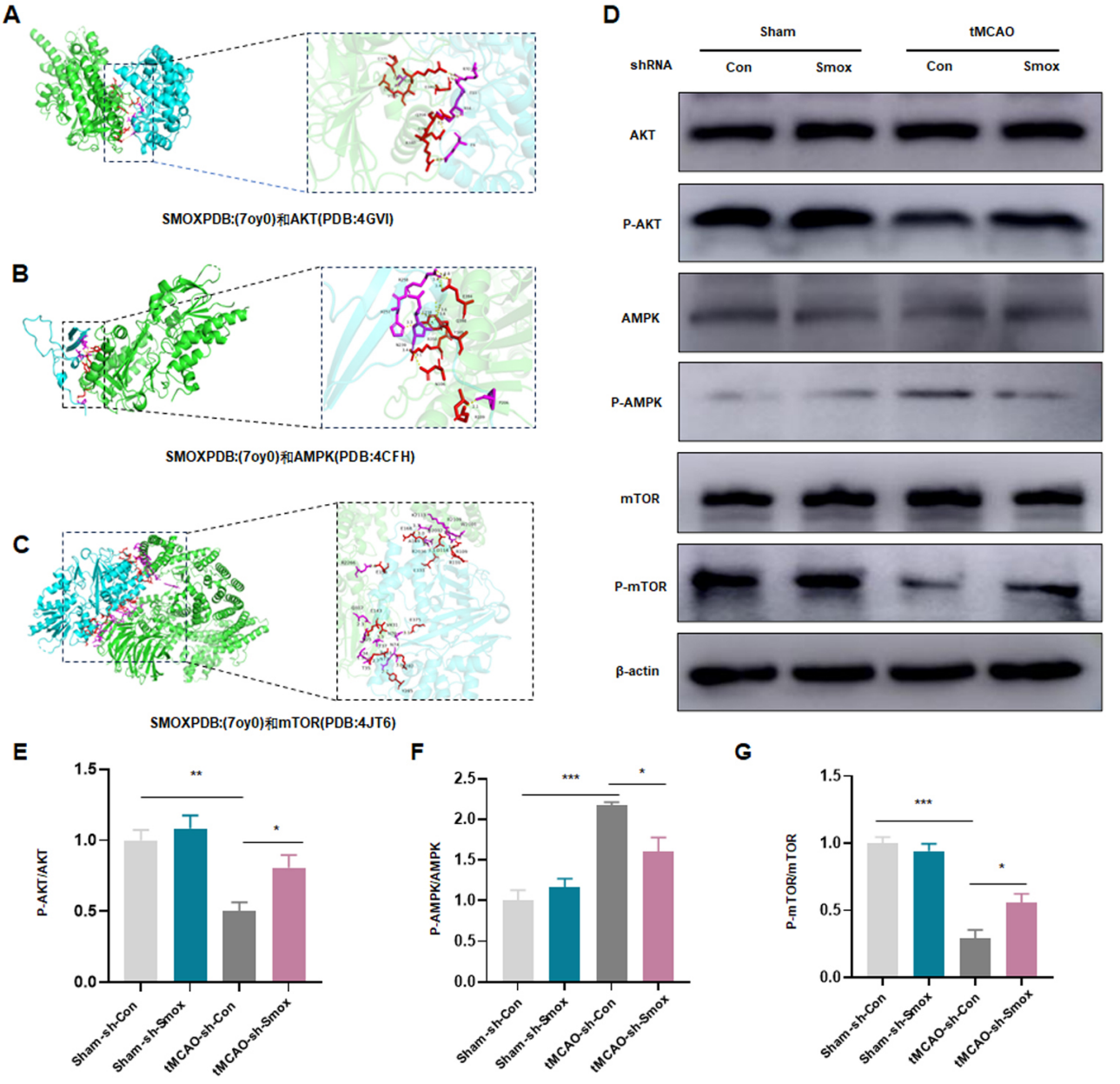


**Fig. 7. Silencing of Smox increased the phosphorylation of AKT and mTOR, but decreased the phosphorylation of AMPK after tMCAO injury**. (A) Molecular dynamic simulation (left panel) and docking (right panel) of AKT (PDB: 4GVI). (B) Molecular dynamic simulation (left panel) and docking (right panel) of AMPK (PDB: 4CFH). (C) Molecular dynamic simulation (left panel) and docking (right panel) of mTOR (PDB: 4JT6). (D) Representative images of p-AMPK, p-AKT, and p-mTOR expression, as detected by Western blot in tMCAO. (E–G) Quantification of the relative expression of p-AMPK, p-AKT, and p-mTOR. $n = 3$. $^{*}p < 0.05$, $^{**}p < 0.01$, and $^{***}p < 0.001$. AMPK, AMP-activated protein kinase; AKT, protein kinase B; mTOR, mechanistic target of rapamycin.

in OGD/R models with silenced Smox. Western blot analysis was employed to quantify the autophagy-related proteins Beclin1, LC3B II/I, and p62 in OGD/R models with silenced Smox (Fig. 8E–H, the original Western blot images are available in the **Supplementary Materials**). Preconditioning with GSK690693 effectively prevented the decrease in Beclin1 and LC3B II/I expression, as well as the increase in p62 levels induced by sh-Smox in the OGD/R models. Additionally, GSK690693 preconditioning mitigated the decrease in Bax and increase in Bcl-2 induced by sh-Smox in OGD/R models (Fig. 8I,J). Overall, the results suggest the protective mechanism of Smox silencing against OGD/R involves the phosphorylation pathway for AKT/AMPK/mTOR in HT22 cells.

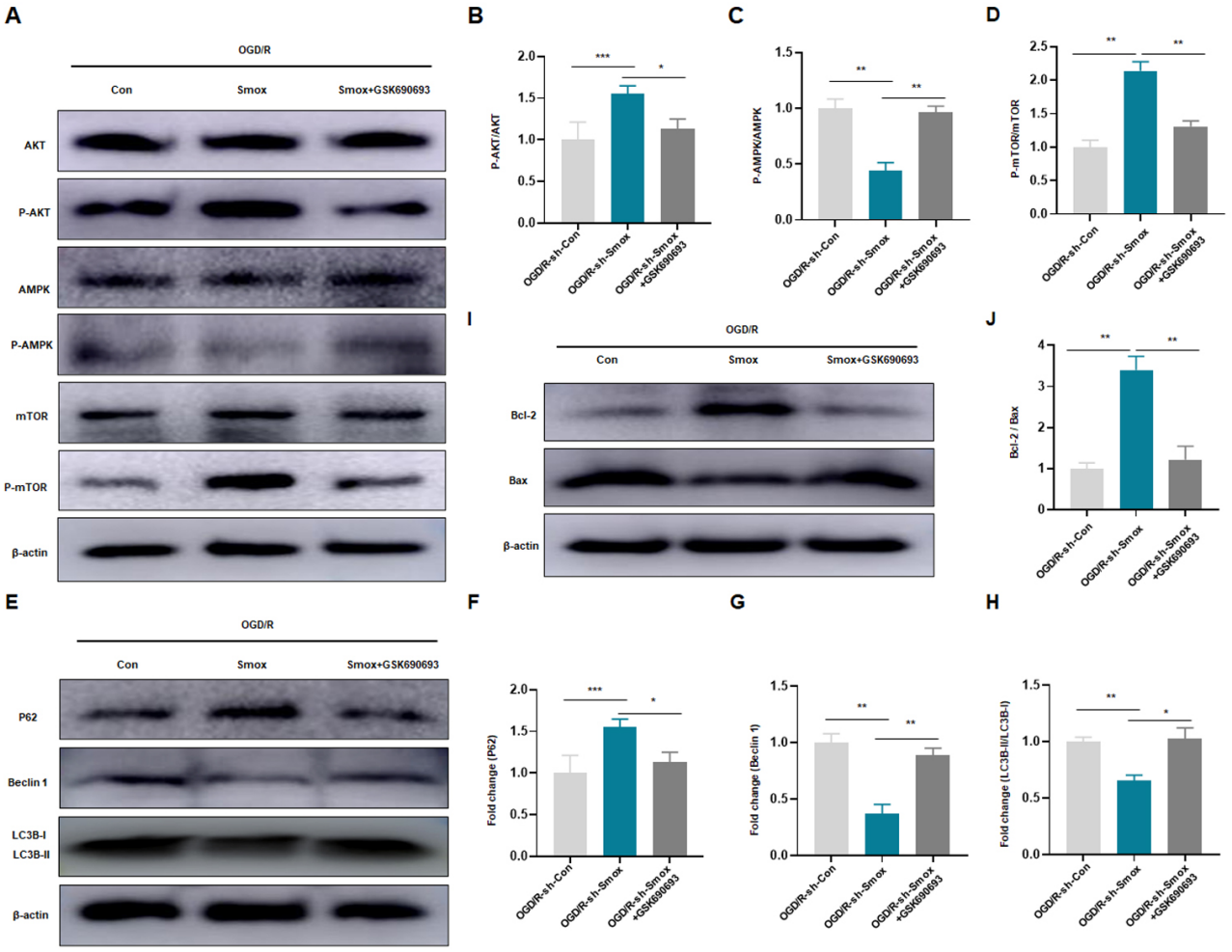


**Fig. 8. Silencing of Smox suppresses autophagy and modulates the AKT/AMPK/mTOR phosphorylation pathway in OGD/R-challenged HT22 cells**. (A) Representative expression of p-AMPK, p-AKT, and p-mTOR detected by Western blot in vitro. (B) Quantified relative expression of p-AKT (C) Quantified relative expression of p-AMPK (D) Quantified relative expression of p-mTOR. $n = 3$ per group. (E) The expression of p62 (F), Beclin1 (G) and LC3B II/I (H), as assessed by Western blot assay. $n = 3$ per group. (I,J) The expression of Bax and Bcl-2, as assessed by Western blot assay. $n = 3$ per group. $^{*}p < 0.05$, $^{**}p < 0.01$, and $^{***}p < 0.001$.

## 4. Discussion

Stroke is a leading cause of disability and death worldwide, often leading to neuronal destruction and altered autophagy [40,41,42]. The current study explored the role of Smox in ischemic injury using a mouse tMCAO model, as well as HT22 cell models exposed to OGD/R. Our findings show that silencing of Smox can protect neurons from ischemic injury in both *in vitro* and *in vivo* settings. Moreover, the neuroprotective effects of Smox knockdown in alleviating neuronal dysfunction are linked to the inhibition of autophagic activation. Mechanistically, Smox regulates autophagy via the AKT/AMPK/mTOR phosphorylation pathway. Taken together, our findings suggest that Smox may exert neuroprotective properties by inhibiting autophagy in an AKT/AMPK/mTOR phosphorylation-dependent manner.

Smox is recognized as a crucial catabolic enzyme involved in polyamine metabolism. It can be readily induced by various stimuli, leading to decreased intracellular spermine levels [43,44]. Although the mechanism underlying Smox expression in stroke remains unclear, previous studies have shown significant decreases in *Smox* mRNA levels and spermine content in fibrotic kidneys following ischemia-reperfusion injury at day 21 [45]. This suggests a potential role for Smox in ischemic conditions, although its specific functions in stroke warrant further investigation.

Additionally, Smox is upregulated during infections and has been linked to an increased risk of cancer in humans. In an *H. pylori*-induced mouse model of gastric cancer, genetic deletion of Smox was found to inhibit tumor progression. Smox-deficient mice exhibit reduced expression of pro-inflammatory and pro-carcinogenic genes, lower cell proliferation, and less DNA damage. Moreover,

acrolein, a highly reactive electrophile generated during infection with *H. pylori* in both human and mouse gastric epithelial cells, shows diminished production when Smox is deleted or inhibited [26]. Studies involving various Smox-overexpressing transgenic mice and excitotoxicity models have shown that elevated Smox levels disturb polyamine homeostasis, thereby exacerbating the severity of seizures induced by kainic acid and pentylentetrazole [46,47]. Additionally, the Smox reaction products of spermidine and spermine have been identified as potent autophagy agonists, thus suggesting potential direct links between Smox and autophagy [48,49,50]. Knocdown of Smox has also been shown to protect against renal fibrosis by increasing autophagy activity and reducing cell senescence [24].

Autophagy is essential for neuronal protection by digesting damaged organelles, thereby averting apoptosis and producing energy. This postpones ion imbalance and necrosis after cerebral ischemia and hypoxia [40,51]. The current research provides substantial evidence that Smox expression is markedly increased after tMCAO and OGD/R injury in HT22 cells, indicating a potential crucial role in neuronal reperfusion injury. LC3B is an essential protein in autophagosome production and serves as a marker to assess the autophagy level in cells [52,53]. The autophagy marker p62 serves as a connector between LC3B and polyubiquitinated proteins. During the development of autophagosomes, p62 is selectively integrated into autophagosomes and subsequently destroyed by proteolytic enzymes contained within autolysosomes. p62 is therefore an essential factor during autophagy degradation, and its expression is inversely linked to autophagy activity [52,54,55]. In the current study, reduced levels of autophagy-related markers were observed following shRNA-mediated Smox knockdown, concomitant with elevated protein levels of anti-apoptotic Bcl-2 and p62. Silencing of Smox appears to have protective effects during reperfusion injury by markedly reducing OGD/R-induced autophagy and apoptosis in tMCAO and HT22 cells (Figs. 3,4,5). In the tMCAO animal model of cerebral injury, treatment with the autophagy agonist rapamycin was observed to increase infarct volume, exacerbate neuronal damage, and delay the recovery of motor function [56]. Conversely, the enhancement of autophagy with 3-MA has been reported to reduce cerebral ischemia-reperfusion injury [21]. Our research with the OGD/R model and Smox knockdown is consistent with these earlier findings by demonstrating reduced LC3B expression and elevated NeuN expression. The knockdown of Smox by 3-MA further diminishes neuronal death and drastically lowers LC3B expression (Fig. 6).

Basal autophagy in neurons helps to maintain homeostasis by eliminating surplus organelles, promoting the turnover of aggregates, and supplying metabolic substrates required for cell survival. However, persistent or excessive autophagy can result in degradation of essential cell components and survival factors, leading to metabolic depletion, DNA damage, and activation of neuronal apoptosis and necrosis pathways [40]. Effective regulation of autophagy likely depends on precise modulation of the autophagy signaling system, through either inhibition or stimulation. Multiple studies have associated the AMPK/mTOR signaling pathway with autophagy [57], underscoring its potentially essential function in ischemic stroke [58]. The activation of mTOR was shown to be suppressed by p-AMPK [59]. A previous study showed that epigallocatechin-3-gallate (EGCG) alleviates tMCAO by inhibiting autophagy through the AKT/AMPK/mTOR phosphorylation pathway [11]. The AKT/mTOR signaling pathway is crucial for modulating inflammation, and especially for the control of autophagy [60,61,62,63]. Activation of this pathway has been shown to inhibit autophagy [64]. Activation of AKT/mTOR also mitigates brain injury resulting from stroke [65,66]. In the current study, we explored the role of AKT/AMPK/mTOR in the neuroprotective effects conferred by Smox knockdown in stroke by employing GSK690693 to inhibit AKT/AMPK activity. We subsequently assessed autophagy and the expression of apoptosis factors, as well as evaluating OGD/R-induced injury in HT22 cells. Western blot analysis revealed reduced levels of p-AKT and p-mTOR protein expression, coupled with elevated p-AMPK in the tMCAO group. Conversely, Smox knockdown increased the levels of p-AKT and p-mTOR, while reducing the levels of p-AMPK following a stroke. In vitro results indicated that AKT/AMPK/mTOR inhibition with GSK690693 markedly reversed the effects on autophagy and apoptosis (Fig. 8). Our results suggest the AKT/AMPK/mTOR signaling pathway is essential for the neuroprotective and inhibitory effects of Smox knockdown on autophagy in tMCAO-induced cerebral damage. As a key enzyme in polyamine metabolism, Smox catalyzes the production of metabolites that may regulate the phosphorylation of AMPK, Akt, and mTOR through oxidative stress and metabolic signaling. Previous studies have demonstrated clear crosstalk between polyamine metabolism and energy-sensing pathways; for instance, polyamine metabolism-related molecules can modulate AMPK signaling activity [49]. Overall, these results suggest that altered expression of Smox may regulate the AKT/AMPK/mTOR signaling axis by affecting the intracellular redox balance and AMP/ATP ratio.

Our study has several limitations. First, the *in vitro* experiments were performed using the HT22 cell line, which, although widely used in cerebral ischemia research, is an immortalized cell line that does not fully represent mature neurons or capture the complex multicellular interactions (neurons, astrocytes, microglia, endothelial cells) involved in ischemic brain injury. Second, the connection between Smox and the AKT/AMPK/mTOR pathway remains indirect. Pathway regulation was inferred from phosphorylation changes and pharmacological interventions, which do not exclude indirect effects. Molecular docking pro-

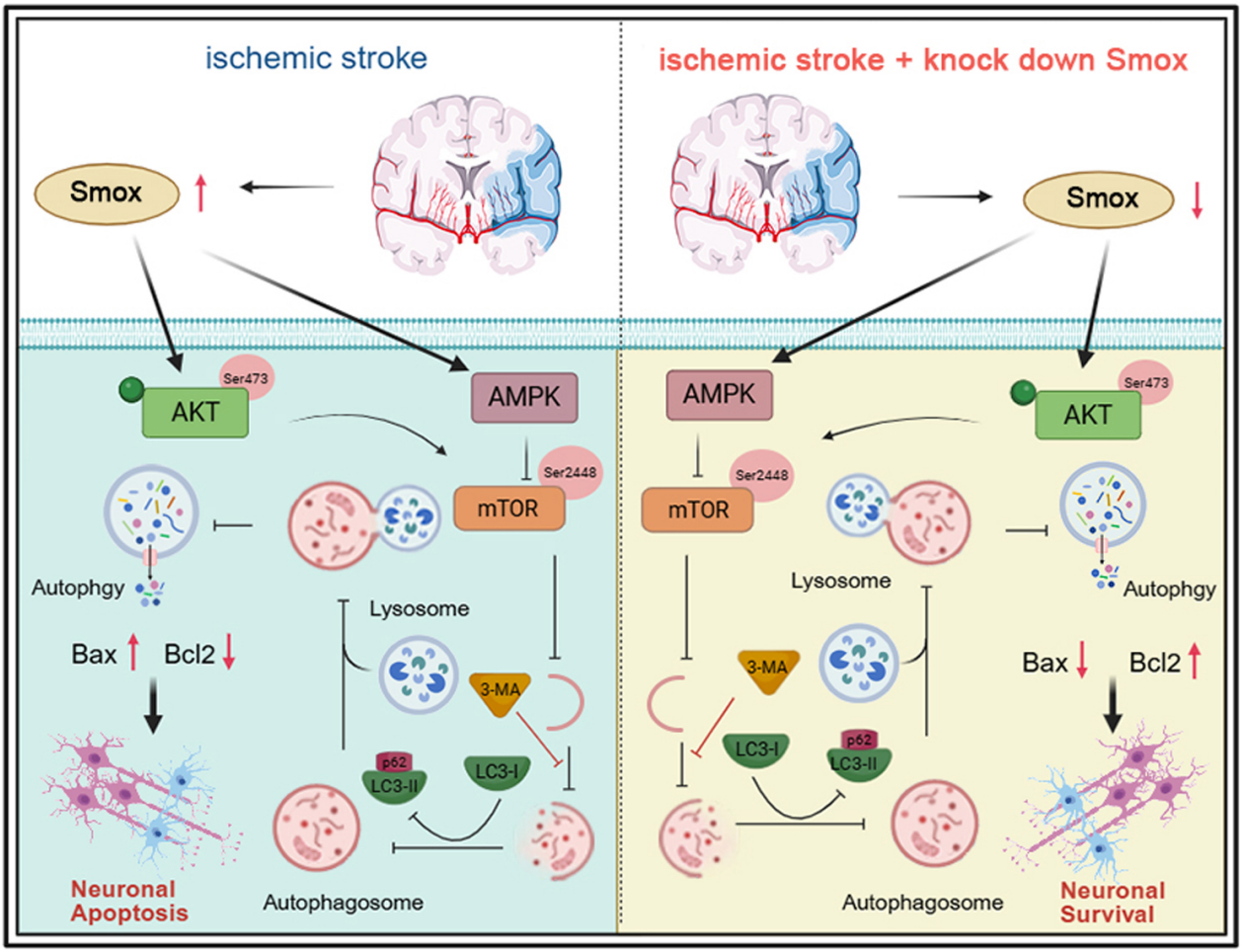


**Fig. 9. Silencing of Smox protects against stroke by suppressing neuronal autophagy through a molecular mechanism involving the AKT/AMPK/mTOR phosphorylation pathway**.

vided computational clues, but it does not validate biological interactions. Smox is known to be a vital enzyme in polyamine metabolism and its activity also modulates ROS levels. Given the established crosstalk between polyamine metabolism, oxidative stress, and energy-sensing pathways [67,68], we propose that Smox regulates this pathway indirectly through ROS-induced oxidative stress rather than through direct physical binding. Third, the autophagy data should be interpreted with caution. Although LC3B, Beclin1, p62, and transmission electron microscopy are commonly used markers for autophagy, they have limitations in distinguishing between increased autophagic activity and altered autophagic flux. p62 accumulation may result from impaired degradation [69] or transcriptional changes [70], while decreased LC3B levels may indicate suppression of initiation or adaptive changes following flux blockade [71]. Taken together, the conclusion that Smox knockdown suppresses autophagy is considered reasonable and reliable within the current experimental system.

## 5. Conclusions

In conclusion, our findings indicate the neuroprotective effects of Smox knockdown in stroke are linked to autophagy suppression via the AKT/AMPK/mTOR phosphorylation pathway (Fig. 9). Our results bring novel insights into the processes by which Smox knockdown affects autophagy and cerebral ischemia injury, potentially facilitating the development of more effective treatment options for stroke.

## Availability of Data and Materials

Data will be made available from the corresponding author on request.

## Author Contributions

Study design: GW, ZL, QW, ZF and ZZ; manuscript composition: GW, ZL, QW, and ZZ; experimental execution: GW, ZL, PL, KM, YW, MY, ZG, HW; data analysis: HL, LL, LJ, and YC. All authors contributed to editorial changes in the manuscript. All authors read and approved

the final manuscript. All authors have participated sufficiently in the work and agreed to be accountable for all aspects of the work.

## Ethics Approval and Consent to Participate

This study was approved by the Animal Ethics Committee of Fourth Affiliated Hospital of Harbin Medical University (Approval ID: 2025-DWSYLLC2-34). The study was conducted in accordance with the local legislation and institutional requirements, and followed the National Institutes of Health Guide for the Care and Use of Laboratory Animals.


## Acknowledgment

Not applicable.

## Funding

This research received funding from the National Natural Science Foundation of China (82104147), the Heilongjiang Provincial Natural Science Foundation (PL2024H146), and the Zhuhai Social Development Science and Technology Plan Project (2420004000201).


## Conflicts of Interest

The authors declare no conflicts of interest.

## Supplementary Material

Supplementary material associated with this article can be found, in the online version, at https://doi.org/10.31083/JIN50711.

## References


[1] Xu Z, Li Y, Pi P, Yi Y, Tang H, Zhang Z, et al. B. glomerulata promotes neuroprotection against ischemic stroke by inhibiting apoptosis through the activation of PI3K/AKT/mTOR pathway. Phytomedicine : International Journal of Phytotherapy and Phytopharmacology. 2024; 132: 155817. https://doi.org/10.1016/j.phymed.2024.155817

[2] Ren X, Hu H, Farooqi I, Simpkins JW. Blood substitution therapy rescues the brain of mice from ischemic damage. Nature Communications. 2020; 11: 4078. https://doi.org/10.1038/s41467-020-17930-x

[3] Liu Q, Johnson EM, Lam RK, Wang Q, Bo Ye H, Wilson EN, et al. Peripheral TREM1 responses to brain and intestinal immunogens amplify stroke severity. Nature Immunology. 2019; 20: 1023–1034. https://doi.org/10.1038/s41590-019-0421-2

[4] Ho JP, Powers WJ. Contemporary Management of Acute Ischemic Stroke. Annual Review of Medicine. 2025; 76: 417–429. https://doi.org/10.1146/annurev-med-050823-094312

[5] Lin L, Ba Z, Tian H, Qin H, Chen X, Zhou X, et al. Ultrasound-responsive theranostic platform for the timely monitoring and efficient thrombolysis in thrombi of tPA resistance. Nature Communications. 2024; 15: 6610. https://doi.org/10.1038/s41467-024-50741-y

[6] Xu X, Gao W, Li L, Hao J, Yang B, Wang T, et al. Annexin A1 protects against cerebral ischemia-reperfusion injury by modulating microglia/macrophage polarization via FPR2/ALX-dependent AMPK-mTOR pathway. Journal of Neuroinflammation. 2021; 18: 119. https://doi.org/10.1186/s12974-021-02174-3

[7] Tu Y, Peng J, Gong X, Zhu P, Zhang C, Liu Y, et al. Association Between Enlarged Perivascular Spaces and Early Acute Ischemic Stroke with Cognitive Impairment: A Cross-Sectional Study. Journal of Integrative Neuroscience. 2024; 23: 187. https://doi.org/10.31083/j.jin2310187

[8] Zang N, Lin Z, Huang K, Pan Y, Wu Y, Wu Y, et al. Biomarkers of Unfavorable Outcome in Acute Ischemic Stroke Patients with Successful Recanalization by Endovascular Thrombectomy. Cerebrovascular Diseases (Basel, Switzerland). 2020; 49: 583–592. https://doi.org/10.1159/000510804

[9] Wang Z, Liu Y. Red Cell Distribution Width and Futile Recanalization in Individuals with Acute Ischemic Stroke following Endovascular Treatment. Journal of Integrative Neuroscience. 2023; 22: 78. https://doi.org/10.31083/j.jin2203078

[10] Mao R, Zong N, Hu Y, Chen Y, Xu Y. Neuronal Death Mechanisms and Therapeutic Strategy in Ischemic Stroke. Neuroscience Bulletin. 2022; 38: 1229–1247. https://doi.org/10.1007/s12264-022-00859-0

[11] Wang L, Dai M, Ge Y, Chen J, Wang C, Yao C, et al. EGCG protects the mouse brain against cerebral ischemia/reperfusion injury by suppressing autophagy via the AKT/AMPK/mTOR phosphorylation pathway. Frontiers in Pharmacology. 2022; 13: 921394. https://doi.org/10.3389/fphar.2022.921394

[12] He Z, Ning N, Zhou Q, Khoshnam SE, Farzaneh M. Mitochondria as a therapeutic target for ischemic stroke. Free Radical Biology & Medicine. 2020; 146: 45–58. https://doi.org/10.1016/j.freeradbiomed.2019.11.005

[13] Zhou B, Wang H, Zhang B, Zhang L. Licochalcone B attenuates neuronal injury through anti-oxidant effect and enhancement of Nrf2 pathway in MCAO rat model of stroke. International Immunopharmacology. 2021; 100: 108073. https://doi.org/10.1016/j.intimp.2021.108073

[14] Liu A, Hu J, Yeh TS, Wang C, Tang J, Huang X, et al. Neuroprotective Strategies for Stroke by Natural Products: Advances and Perspectives. Current Neuropharmacology. 2023; 21: 2283–2309. https://doi.org/10.2174/1570159X21666230717144752

[15] Zhang DM, Zhang T, Wang MM, Wang XX, Qin YY, Wu J, et al. TIGAR alleviates ischemia/reperfusion-induced autophagy and ischemic brain injury. Free Radical Biology & Medicine. 2019; 137: 13–23. https://doi.org/10.1016/j.freeradbiomed.2019.04.002

[16] Ajoolabady A, Wang S, Kroemer G, Penninger JM, Uversky VN, Pratico D, et al. Targeting autophagy in ischemic stroke: From molecular mechanisms to clinical therapeutics. Pharmacology & Therapeutics. 2021; 225: 107848. https://doi.org/10.1016/j.pharmthera.2021.107848

[17] Yu S, Qin Z, Chen Y, Wang F, Li Z, Huang R, et al. Antimony-induced hippocampal neuronal impairment through ferroptosis activation from NCOA4-mediated ferritinophagy. Chemico-biological Interactions. 2025; 409: 111415. https://doi.org/10.1016/j.cbi.2025.111415

[18] Li Y, Yin Q, Wang B, Shen T, Luo W, Liu T. Preclinical reserpine models recapitulating motor and non-motor features of Parkinson's disease: Roles of epigenetic upregulation of alpha-synuclein and autophagy impairment. Frontiers in Pharmacology. 2022; 13: 944376. https://doi.org/10.3389/fphar.2022.944376

[19] Ahsan A, Liu M, Zheng Y, Yan W, Pan L, Li Y, et al. Natural compounds modulate the autophagy with potential implication of stroke. Acta Pharmaceutica Sinica. B. 2021; 11: 1708–1720. https://doi.org/10.1016/j.apsb.2020.10.018

[20] Shademan B, Avci CB, Karamad V, Soureh GJ, Olia JBH, Esmaily F, et al. The Role of Mitochondrial Biogenesis in Ischemic Stroke. Journal of Integrative Neuroscience. 2023; 22: 88. https://doi.org/10.31083/j.jin2204088

[21] Xing S, Zhang Y, Li J, Zhang J, Li Y, Dang C, et al. Beclin 1 knockdown inhibits autophagic activation and prevents the secondary neurodegenerative damage in the ipsilateral thalamus following focal cerebral infarction. Autophagy. 2012; 8: 63–76. https://doi.org/10.4161/auto.8.1.18217

[22] Proietti E, Rossini S, Grohmann U, Mondanelli G. Polyamines and Kynurenines at the Intersection of Immune Modulation. Trends in Immunology. 2020; 41: 1037–1050. https://doi.org/10.1016/j.it.2020.09.007

[23] Holbert CE, Cullen MT, Casero RA, Jr, Stewart TM. Polyamines in cancer: integrating organismal metabolism and antitumour immunity. Nature Reviews. Cancer. 2022; 22: 467–480. https://doi.org/10.1038/s41568-022-00473-2

[24] Luo D, Lu X, Li H, Li Y, Wang Y, Jiang S, et al. The Spermine Oxidase/Spermine Axis Coordinates ATG5-Mediated Autophagy to Orchestrate Renal Senescence and Fibrosis. Advanced Science (Weinheim, Baden-Wurttemberg, Germany). 2024; 11: e2306912. https://doi.org/10.1002/advs.202306912

[25] Amin M, Tang S, Shalamanova L, Taylor RL, Wylie S, Abdullah BM, et al. Polyamine biomarkers as indicators of human disease. Biomarkers : Biochemical Indicators of Exposure, Response, and Susceptibility to Chemicals. 2021; 26: 77–94. https://doi.org/10.1080/1354750X.2021.1875506

[26] McNamara KM, Sierra JC, Latour YL, Hawkins CV, Asim M, Williams KJ, et al. Spermine oxidase promotes Helicobacter pylori-mediated gastric carcinogenesis through acrolein production. Oncogene. 2025; 44: 296–306. https://doi.org/10.1038/s41388-024-03218-7

[27] Chaturvedi R, Asim M, Barry DP, Frye JW, Casero RA, Jr, Wilson KT. Spermine oxidase is a regulator of macrophage host response to Helicobacter pylori: enhancement of antimicrobial nitric oxide generation by depletion of spermine. Amino Acids. 2014; 46: 531–542. https://doi.org/10.1007/s00726-013-1531-z

[28] Chaturvedi R, Cheng Y, Asim M, Bussière FI, Xu H, Gobert AP, et al. Induction of polyamine oxidase 1 by Helicobacter pylori causes macrophage apoptosis by hydrogen peroxide release and mitochondrial membrane depolarization. The Journal of Biological Chemistry. 2004; 279: 40161–40173. https://doi.org/10.1074/jbc.M401370200

[29] Chaturvedi R, de Sablet T, Asim M, Piazuelo MB, Barry DP, Verriere TG, et al. Increased Helicobacter pylori-associated gastric cancer risk in the Andean region of Colombia is mediated by spermine oxidase. Oncogene. 2015; 34: 3429–3440. https://doi.org/10.1038/onc.2014.273

[30] Bai Y, Ren H, Leng S, Yuan M, Jiang Y, Zhang S, et al. CD8+GZMK+CD27+CCR7+ T cells mobilized by splenic sympathetic nerves aggravate brain ischemia–reperfusion injury via CCL19-positive endothelial cells. Cellular & Molecular Immunology. 2025; 22: 1061–1076. https://doi.org/10.1038/s41423-025-01311-9

[31] Wang G, Han B, Shen L, Wu S, Yang L, Liao J, et al. Silencing of circular RNA HIPK2 in neural stem cells enhances functional recovery following ischaemic stroke. EBioMedicine. 2020; 52: 102660. https://doi.org/10.1016/j.ebiom.2020.102660

[32] Li B, Xi W, Bai Y, Liu X, Zhang Y, Li L, et al. FTO-dependent m6A modification of Plpp3 in circSCMH1-regulated vascular repair and functional recovery following stroke. Nature Communications. 2023; 14: 489. https://doi.org/10.1038/s41467-023-36008-y

[33] Bai Y, Chang D, Ren H, Ju M, Wang Y, Chen B, et al. Engagement of N6-methyladenisine methylation of Gng4 mRNA in astrocyte dysfunction regulated by CircHECW2. Acta Pharmaceutica Sinica. B. 2024; 14: 1644–1660. https://doi.org/10.1016/j.apsb.2024.01.011

[34] Zhang G, Li Q, Tao W, Qin P, Chen J, Yang H, et al. Sigma-1 receptor-regulated efferocytosis by infiltrating circulating macrophages/microglial cells protects against neuronal impairments and promotes functional recovery in cerebral ischemic stroke. Theranostics. 2023; 13: 543–559. https://doi.org/10.7150/thno.77088

[35] Wang Y, Tian M, Tan J, Pei X, Lu C, Xin Y, et al. Irisin ameliorates neuroinflammation and neuronal apoptosis through integrin αVβ5/AMPK signaling pathway after intracerebral hemorrhage in mice. Journal of Neuroinflammation. 2022; 19: 82. https://doi.org/10.1186/s12974-022-02438-6

[36] Wu F, Han B, Wu S, Yang L, Leng S, Li M, et al. Circular RNA TLK1 Aggravates Neuronal Injury and Neurological Deficits after Ischemic Stroke via miR-335-3p/TIPARP. The Journal of Neuroscience : the Official Journal of the Society for Neuroscience. 2019; 39: 7369–7393. https://doi.org/10.1523/JNEUROSCI.0299-19.2019

[37] Li S, Nie EH, Yin Y, Benowitz LI, Tung S, Vinters HV, et al. GDF10 is a signal for axonal sprouting and functional recovery after stroke. Nature Neuroscience. 2015; 18: 1737–1745. https://doi.org/10.1038/nn.4146

[38] Hines DJ, Haydon PG. Inhibition of a SNARE-sensitive pathway in astrocytes attenuates damage following stroke. The Journal of Neuroscience : the Official Journal of the Society for Neuroscience. 2013; 33: 4234–4240. https://doi.org/10.1523/JNEUROSCI.5495-12.2013

[39] Wang G, Li Z, Lin P, Zhang H, Wang Y, Zhang T, et al. Knockdown of Smox protects the integrity of the blood-brain barrier through antioxidant effect and Nrf2 pathway activation in stroke. International Immunopharmacology. 2024; 126: 111183. https://doi.org/10.1016/j.intimp.2023.111183

[40] Wu Y, Li Z, Ding T, Yang Y, Wei C, Zhang S, et al. Bidirectional regulation of neuronal autophagy in ischemic stroke: Mechanisms and therapeutic potential. Ageing Research Reviews. 2025; 111: 102842. https://doi.org/10.1016/j.arr.2025.102842

[41] Yang M, Liu B, Chen B, Shen Y, Liu G. Cerebral ischemia-reperfusion injury: mechanisms and promising therapies. Frontiers in Pharmacology. 2025; 16: 1613464. https://doi.org/10.3389/fphar.2025.1613464

[42] Li J, Shen S, Shen H. Heat-shock protein A12A attenuates oxygen-glucose deprivation/reoxygenation-induced human brain microvascular endothelial cell dysfunction via PGC-1α/SIRT3 pathway. Drug Development Research. 2024; 85: e22130. https://doi.org/10.1002/ddr.22130

[43] Vujcic S, Diegelman P, Bacchi CJ, Kramer DL, Porter CW. Identification and characterization of a novel flavin-containing spermine oxidase of mammalian cell origin. The Biochemical Journal. 2002; 367: 665–675. https://doi.org/10.1042/BJ20020720

[44] Vujcic S, Liang P, Diegelman P, Kramer DL, Porter CW. Genomic identification and biochemical characterization of the mammalian polyamine oxidase involved in polyamine back-conversion. The Biochemical Journal. 2003; 370: 19–28. https://doi.org/10.1042/BJ20021779

[45] Sieckmann T, Schley G, Ögel N, Kelterborn S, Boivin FJ, Fähling M, et al. Strikingly conserved gene expression changes of polyamine regulating enzymes among various forms of acute and chronic kidney injury. Kidney International. 2023; 104: 90–107. https://doi.org/10.1016/j.kint.2023.04.005

[46] Zahedi K, Brooks M, Barone S, Rahmati N, Murray Stewart T, Dunworth M, et al. Ablation of polyamine catabolic enzymes provokes Purkinje cell damage, neuroinflammation, and severe ataxia. Journal of Neuroinflammation. 2020; 17: 301. https://doi.org/10.1186/s12974-020-01955-6

[47] Pietropaoli S, Leonetti A, Cervetto C, Venturini A, Mastrantonio R, Baroli G, et al. Glutamate Excitotoxicity Linked to Spermine Oxidase Overexpression. Molecular Neurobiology. 2018; 55: 7259–7270. https://doi.org/10.1007/s12035-017-0864-0

[48] Zhou S, Gu J, Liu R, Wei S, Wang Q, Shen H, et al. Spermine Alleviates Acute Liver Injury by Inhibiting Liver-Resident Macrophage Pro-Inflammatory Response Through ATG5-Dependent Autophagy. Frontiers in Immunology. 2018; 9: 948. https://doi.org/10.3389/fimmu.2018.00948
[49] Zhang X, Zhang L, Chen Z, Li S, Che B, Wang N, et al. Exogenous spermine attenuates diabetic kidney injury in rats by inhibiting AMPK/mTOR signaling pathway. International Journal of Molecular Medicine. 2021; 47: 27. https://doi.org/10.3892/ijmm.2021.4860
[50] Duan Q, Yang W, Jiang D, Tao K, Dong A, Cheng H. Spermine ameliorates ischemia/reperfusion injury in cardiomyocytes via regulation of autophagy. American Journal of Translational Research. 2016; 8: 3976–3985.
[51] Stoka V, Turk V, Turk B. Lysosomal cathepsins and their regulation in aging and neurodegeneration. Ageing Research Reviews. 2016; 32: 22–37. https://doi.org/10.1016/j.arr.2016.04.010
[52] Liu Y, Yao Y, Tao W, Liu F, Yang S, Zhao A, et al. Coenzyme Q10 ameliorates BPA-induced apoptosis by regulating autophagy-related lysosomal pathways. Ecotoxicology and Environmental Safety. 2021; 221: 112450. https://doi.org/10.1016/j.ecoenv.2021.112450
[53] Zhang R, Zhu Z, Ma Y, Tang T, Wu J, Huang F, et al. Rhizoma Alismatis Decoction improved mitochondrial dysfunction to alleviate SASP by enhancing autophagy flux and apoptosis in hyperlipidemia acute pancreatitis. Phytomedicine : International Journal of Phytotherapy and Phytopharmacology. 2024; 129: 155629. https://doi.org/10.1016/j.phymed.2024.155629
[54] Zhu P, Qian J, Xu Z, Meng C, Liu J, Shan W, et al. Piperlonguminine and Piperine Analogues as TrxR Inhibitors that Promote ROS and Autophagy and Regulate p38 and Akt/mTOR Signaling. Journal of Natural Products. 2020; 83: 3041–3049. https://doi.org/10.1021/acs.jnatprod.0c00599
[55] Nie J, Mao Z, Zeng X, Zhao X. Rapamycin protects Sertoli cells against BPA-induced autophagy disorders. Food and Chemical Toxicology : an International Journal Published for the British Industrial Biological Research Association. 2024; 186: 114510. https://doi.org/10.1016/j.fct.2024.114510
[56] Yue Y, Chen P, Ren C. Piezo1 Modulates Neuronal Autophagy and Apoptosis in Cerebral Ischemia-Reperfusion Injury Through the AMPK-mTOR Signaling Pathway. Neurochemical Research. 2024; 50: 32. https://doi.org/10.1007/s11064-024-04291-w
[57] Ha J, Guan KL, Kim J. AMPK and autophagy in glucose/glycogen metabolism. Molecular Aspects of Medicine. 2015; 46: 46–62. https://doi.org/10.1016/j.mam.2015.08.002
[58] Jiang S, Li T, Ji T, Yi W, Yang Z, Wang S, et al. AMPK: Potential Therapeutic Target for Ischemic Stroke. Theranostics. 2018; 8: 4535–4551. https://doi.org/10.7150/thno.25674
[59] Leech T, Chattipakorn N, Chattipakorn SC. The beneficial roles of metformin on the brain with cerebral ischaemia/reperfusion injury. Pharmacological Research. 2019; 146: 104261. https://doi.org/10.1016/j.phrs.2019.104261
[60] Wang C, Li Y, Zhang Y, Smerin D, Gu L, Jiang S, et al. Triolein alleviates ischemic stroke brain injury by regulating autophagy and inflammation through the AKT/mTOR signaling pathway. Molecular Medicine (Cambridge, Mass.). 2024; 30: 242. https://doi.org/10.1186/s10020-024-00995-5
[61] Fang S, Wan X, Zou X, Sun S, Hao X, Liang C, et al. Arsenic trioxide induces macrophage autophagy and atheroprotection by regulating ROS-dependent TFEB nuclear translocation and AKT/mTOR pathway. Cell Death & Disease. 2021; 12: 88. https://doi.org/10.1038/s41419-020-03357-1
[62] Xu X, Su YL, Shi JY, Lu Q, Chen C. MicroRNA-17-5p Promotes Cardiac Hypertrophy by Targeting Mfn2 to Inhibit Autophagy. Cardiovascular Toxicology. 2021; 21: 759–771. https://doi.org/10.1007/s12012-021-09667-w
[63] Zhou T, Ye Y, Chen W, Wang Y, Ding L, Liu Y, et al. Glaucocalyxin A alleviates ulcerative colitis by inhibiting PI3K/AKT/mTOR signaling. Scientific Reports. 2025; 15: 6556. https://doi.org/10.1038/s41598-025-91358-5
[64] Huang L, Chen Y, Liu R, Li B, Fei X, Li X, et al. P-Glycoprotein Aggravates Blood Brain Barrier Dysfunction in Experimental Ischemic Stroke by Inhibiting Endothelial Autophagy. Aging and Disease. 2022; 13: 1546–1561. https://doi.org/10.14336/AD.2022.0225
[65] Li R, Zheng Y, Zhang J, Zhou Y, Fan X. Gomisin N attenuated cerebral ischemia-reperfusion injury through inhibition of autophagy by activating the PI3K/AKT/mTOR pathway. Phytomedicine : International Journal of Phytotherapy and Phytopharmacology. 2023; 110: 154644. https://doi.org/10.1016/j.phymed.2023.154644
[66] Zheng M, Zhou M, Chen M, Lu Y, Shi D, Wang J, et al. Neuroprotective Effect of Daidzein Extracted From Pueraria lobate Radix in a Stroke Model Via the Akt/mTOR/BDNF Channel. Frontiers in Pharmacology. 2022; 12: 772485. https://doi.org/10.3389/fphar.2021.772485
[67] Schibalski RS, Shulha AS, Tsao BP, Palygin O, Ilatovskaya DV. The role of polyamine metabolism in cellular function and physiology. American Journal of Physiology. Cell Physiology. 2024; 327: C341–C356. https://doi.org/10.1152/ajpcell.00074.2024
[68] Fan J, Chen M, Wang X, Tian Z, Wang J, Fan D, et al. Targeting Smox Is Neuroprotective and Ameliorates Brain Inflammation in Cerebral Ischemia/Reperfusion Rats. Toxicological Sciences : an Official Journal of the Society of Toxicology. 2019; 168: 381–393. https://doi.org/10.1093/toxsci/kfy300
[69] Komatsu M, Waguri S, Koike M, Sou YS, Ueno T, Hara T, et al. Homeostatic levels of p62 control cytoplasmic inclusion body formation in autophagy-deficient mice. Cell. 2007; 131: 1149–1163. https://doi.org/10.1016/j.cell.2007.10.035
[70] Hill D, Cosgarea I, Reynolds N, Lovat P, Armstrong J. Research Techniques Made Simple: Analysis of Autophagy in the Skin. The Journal of Investigative Dermatology. 2021; 141: 5–9.e1. https://doi.org/10.1016/j.jid.2020.10.004
[71] Klionsky DJ, Abdel-Aziz AK, Abdelfatah S, Abdellatif M, Abdoli A, Abel S, et al. Guidelines for the use and interpretation of assays for monitoring autophagy (4th edition)1. Autophagy. 2021; 17: 1–382. https://doi.org/10.1080/15548627.2020.1797280